

# HUMAN POWER

THE TECHNICAL JOURNAL OF THE IHPVA  
VOL. 6 NO. 1  
SPRING, 1987

ISSUE NO. 19

## The 20-knot Human-Powered Water Craft

*(HP is reprinting, in parts, Alec Brooks' paper on high-speed hydrofoils, which was given at the Third IHPVA Scientific Symposium. It has been in great demand. As a result of this paper, the article in the SCIENTIFIC AMERICAN in December 1986, and demonstrations by and interviews of Allan Abbott and Alec Brooks on TV and other media, including an appearance on Australian television in a program called "Beyond 2000", individuals, groups and universities around the world are working feverishly on human-powered hydrofoils. I asked Alec on April 16 what developments there had been since the Vancouver EXPO races and symposium in September 1986, and he said that Allan and he had been doing a little development by testing their two Flying Fishes against each other; that two commercial companies were discussing possible production; and that they were preparing for a June assault on the 2000-m record with Steve Hegg providing the power. -- Dave Wilson)*

### Abstract

Until now, the fastest human-powered water craft have been the long narrow oared shells, powered by crews of between one and eight rowers. Recent developments in hydrofoil and propeller design have resulted in several single-rider water craft that are as fast, or faster, than single shells. These craft are in the infancy of their development. With further refinement, single-rider hydrofoils will be faster than oared eights. A method is given for optimum wing sizing, based on structural factors, minimum power, and takeoff speed constraints. The main design parameter is the expected duration of the competition -- this determines how much power is available from the rider. Other design considerations are the takeoff speed and minimum power required. For very short, high-power cases, the optimum design has very small wings and a high takeoff speed, making it impossible to ride at low speeds or low power. High power designs with constraints on minimum power and takeoff speed are explored, showing the associated penalties in top speed. It is shown that below a certain design power level, hydrofoils, while still possible, are less efficient than displacement-hulled craft.

### Introduction

For the past hundred years, the highest-speed human-powered water craft have been the narrow oared racing shells. Under the sanctioning of collegiate rowing organizations, these craft evolved slowly into the elegant craft of today. This evolution has much in common with that of the standard racing bicycle. Both are highly optimized vehicles which evolved under a set of constraints designed to force all vehicles of each class to be largely the same. Under these constraints progress is made, but only in gradual refinements, never in great leaps.

The IHPVA was founded to foster innovation in the design of human-powered vehicles. As a result of the IHPVA, land-vehicle performance has taken a quantum leap in the last decade. Freed of restrictive design rules, designers have developed streamlined land vehicles which are 50 percent faster than standard bicycles. A similar revolution is just beginning in human-powered water vehicles. With the encouragement and sanctioning of the IHPVA, a new wave of watercraft will soon be toppling all existing records held by oared shells, with speed improvements at least as great as those seen for the land vehicles.

*continued on page 8*

### In this issue...

The 20 Knot Human Powered Water Craft, Alec Brooks	1
Editorial Comments, Dave Wilson	2
Letters to Human Power	3
Conception and Optimization of Human Powered Aircraft, E. Schoberl	4 - 14
Dynamic Stability of the Bicycle, Y. Hénaff	15 - 17
Point/Counterpoint, Hénaff, Papadopoulos & Ruina	18 - 19
Build the Flunder, Reiss and Pivitt	20

## EDITORIAL COMMENTS

by David Gordon Wilson

### HUMAN POWER

The Technical Journal of the  
INTERNATIONAL HUMAN-  
POWERED VEHICLE  
ASSOCIATION

David Gordon Wilson, editor  
15 Kennedy Road  
CAMBRIDGE, MA 02138,  
USA

Phones: 617-253-5121 (work)  
617-876-6326 (home)  
Spring 1987 volume 6, no. 1

*HUMAN POWER* is published quarterly by the International Human Powered Vehicle Association, Inc., a non-profit organization devoted to the study and application of human muscular potential to propel craft through the air, in the water and on land. Membership information is available by sending a self-addressed, stamped business-sized envelope to: **IHPVA P.O. Box 51255, Indianapolis, IN 46251-0255 USA.**

Material in *HUMAN POWER* is copyrighted by the IHPVA. Unless copyrighted by the author(s), complete articles or representative excerpts may be published elsewhere if full credit to the author(s) and the IHPVA is prominently given.

This issue of *HUMAN POWER* was typed by Sabina Rataj, Dan Bloom and David Wilson; was set up by Tom Healy and Marti Daily. Printed at Apple Press by Tom Healy. Distributed by Marti Daily and a cast of dozens. Special thanks to translators, including Otto Brodrick, who translated the "Flunder" article.

This issue has been the easiest to put together in the three years of my editorship, mainly because of the very great help of the volunteers named on this page. There has also been another significant development: contributions have been sent to *HUMAN POWER* unsolicited. And they are very good contributions, as I hope you will agree. It is a compliment. The authors feel that *HP* is a worthy publication to carry the fruits of their considerable labors. May the trend continue!

All we need now to advance to the point where we can further improve the scope, size and quality of our journal is a readership in the ten-to-fifty-thousand range. Then we could ease the load on our volunteers and bring in some commercial-advertising income. The IHPVA has been getting many excellent notices in prestigious publications. We need to translate this enthusiasm into IHPVA members. Having the international championships as part of "HUMAN-POWER WEEK" in Washington, D.C. in September, as Marti Daily, Steve Stollman and others are working hard to bring to reality, could be the key to our growth.

### UNRESTRAINED BRACHISTOCHRONES

You may feel that the last diversion you would want in an attempt on the land speed record would be an unrestrained ant, let alone a brachistochrone. You may be wrong. I met the world's expert on these recently at Clark University: David G. Stork, of the physics faculty. He sent me several questions of the following type. Suppose that two HPVs are travelling on a frictionless horizontal plane with the same initial velocity. At point *A* one continues on the plane and arrives at point *B*. The other takes a route that passes into an undulating valley, ending up with a climb to point *B*. Which is going faster at point *B*? Answer: They are moving at the same speed, because there is no mechanism to introduce friction. Which gets there first? Answer: The HPV that went through the valley will always get there first, even though it traverses a longer distance. Why? Because its average velocity along the slope, and its horizontal component of velocity, are higher than that of the HPV on the plane. Therefore it is possible to have an undulating track with a mean slope within IHPVA limits that will have local deviations from the slope and that will give possibly considerable advantages over a track with a constant slope.

David Stork has promised us a summary article on sliding and rolling brachistochrones for a future issue.

### A HISTORY OF THE IHPVA SPEED CHAMPIONSHIPS

Ronald Steven Blair is writing a history of the championships, compiling the rules as they evolved and the currently valid rules, and will later be making the history available for purchase. This is the type of individual enterprise that makes the IHPVA what it is. If anyone has material to contribute, please let Steve know: **275 Castle Hill Ranch Road, Walnut Creek, CA 94595; phone 415-932-6460.** Some time I plan to make an index and a one-page history of *HUMAN POWER*. If anyone has made a start, would s/he please let me know.

### THE FARNSWORTH FORMULA

Jim Farnsworth is a man with a mission: to change the bicycling world. He believes (and I agree with him) that it makes no sense to have a standard crank length for almost all sizes of bicycles. Jim would go further than that: he believes that the crank length should approach half the length of the femur, "The 170-mm crank may be the major cause of knee injuries among cyclists." He is of about average height, and uses cranks a little over 220 mm long. He also believes - as I do - in wide-range gears. He believes that optimum foot speed is better achieved through a large-diameter pedal circle at moderate rpm than with a small-diameter circle at high rpm. One reason is that the dynamic forces, for the same foot speed, go down with increase of radius. Incidentally, long cranks require less of a compromise on a recumbent than on a "regular" ten-speed bike.

Jim Farnsworth lent me the manuscript of an entertainingly written book about his adventures in design and in life. If a publisher were to want to look at it, he would be delighted. Here is his address: **398 Shore Drive, Laconia NH 03246 USA 603-524-1695.**

## LETTERS



## IN THE AIR

The free exchange of ideas is important to R & D, and *HUMAN POWER* does this very well... [I wanted to send a report on a] book on unconventional aircraft... compact circular wings or circular wing types shown in the book might be practical for recreational HPAs. It is *Unconventional Aircraft*, by Peter M. Bowers, Tab Books, Blue Ridge Summit, PA 17214, 1984. [Here is a list of topics:]

Platz sailboat glider; Zanon seed-type aircraft; advantages of tail-less aircraft for hang gliders and ultralights in the 1970s and 1980s; circle-wing biplane; American Nemuth parasol, circular wing; Arup flying wings; Flettner-rotor wing; Lanier Vacuum plane; Custer channel wing; landing gear; ducted propellers; Ben Brown's diamond wing.

Edward G. Sward,  
215 Cambridge St., Worcester,  
MA 01603 USA

## COMMENTS ON "RICKSHAWS"

The first thought that came to my mind after rushing through the piece, *'Rickshaws in Bangladesh'* by Fred Willkie, was that he was saying a lot about everything, and doing it very well. As an advocate for HPUV usage, specifically in non-third-world locales, I felt that his stark accounts of the social and economic realities of rickshaw drivers were relevant to HPUV development in Western countries as well. (Recently, I heard of financially abused delivery drivers in New York City in the Asian-restaurant business).

My own intercultural experiences with HPUV development began in a slightly different culture. Yet somehow, the similarities between his conclusions and my own are not far apart.

While researching and eventually constructing trailers for the distribution of food in Switzerland, I often had a vision of a culture where this transport mode would be developed. It wasn't just a vision of advances in HPUV technical development but included improvements in life, specifically in how we move goods and people.

It seemed as if Asia was the place where HPUVs had become established. Yet after reading of the situation in Bangladesh, it is obvious that a HPUV transport system

is a complex matter. We have much to learn from around the world if we are to create a technically advanced and humane HPUV usage.

There are a few points that Fred Willkie has mentioned that I feel are important for any locale.

## 1. Materials.

I am as interested as the next person in lightening these vehicles and making them more efficient. However, it is easy to feel creatively impotent these days if one isn't using the latest high-tech materials. Use available materials! Many Europeans I contacted utilize recycled materials in their construction of HPUVs. A few pieces of tubing and a wheel - *voila* - a sidecar! And it isn't likely that you will have to melt down old buckles for brazing wire!

## 2. The Social and Economic Context

Unlike Bangladesh, where the motivation to use these vehicles seems to be primarily related to economics, we in Western cultures must emphasize other motivations in advocating HPUVs. So, in the words of Fred Willkie "... have the right questions before you offer answers." For many people will want to know what place these crazy vehicles could have in their lives. Whether it be providing substitute transport methods for the most polluting of urban vehicles, the van and taxi; or for transporting children and handicapped, or for cleaning streets, or...." the fact is that one must consider what will work in the context of people's minds and lives. Development without context is like a bicycle tire in a tram track. Very linear! Thanks Fred Willkie.

Jan Vandertuin  
P.O. Box 573  
South Edgemont, MA 01258 USA

## HP HELICOPTERS

(This was in reply to my letter enquiring about the Nihon University work on HP helicopters Ed.)

...I am only an HPV fan. I am not a member of the Nihon University HP Helicopter (HPH) team. But I did visit Professor Naito at his home, and told him about the twelfth IHPSC. I asked him if he could report on the latest developments on the helicopter. He declined for the following reasons.

1. He succeeded in hovering his HPH for a few seconds several centimeters above

the ground on December, 6, 1985. This was the ninth day of experimentation and the 85th trial flight. The pilot was his student Koichi Nakamura, Japanese champion long-distance hang-glider pilot. Unfortunately, there was no film or tape record of the flight and he feels that he cannot claim the flight without corroboration.

2. After his retirement from Nihon University, there is no successor wanting to carry on his work either at Nihon or elsewhere in Japan.

Toshio Kataoka 914-6 Mamedo Kohuku, Yokomama Kanagawa, Japan 222

(And in a later letter Toshio Kataoka sent a copy of a report of the 12th IHPSC in the leading newspaper *Yomiuri Shinbon* of January 22, 1987, and wrote "Congratulations! World record of HPA of MIT!" He enclosed a couple of color prints, which we may be able to reproduce here -- Dave Wilson.)

## STUDED TIRES

Here is an update on the studded bike tires. On page 14 of *CYCLIST*, April, 1987, there are photographs of a set of tires with #6 pan-head sheet-metal screws and nuts. I have since tried these screws, plus washers under the nuts, in my tires. They are better than those reported in my article in *HP 5/4* because the screws are hardened, and the points are sharp for better traction on ice. I did a quick experiment by grinding two screws side by side. The hardened screw took almost twice as much grinding to remove the same amount of metal. The sheet-metal screws tap their own threads in the nuts, making them a little more difficult to get started, but the finished result gives superior traction and greater durability.

James Donohue, 87 Plymouth Drive North, Glen Head, NY 11545 USA

## FIGURE-EIGHT DRIVE

Thank you for publishing my article about my figure-eight drive in *HUMAN POWER*: it was an honor to present my discovery to our HP group.

Anthony J. Patroni, 9005 Amherst Avenue, Margate NJ 08402 USA

# CONCEPTION AND OPTIMIZATION OF HUMAN-POWERED AIRCRAFT

By E. Schoberl

(This is an edited and shortened version of a paper presented at the twentieth OSTIV-Congress at Benalla, Australia in January, 1987. (It is both a summary of and a sequel to the article on the MUSCULAIR 1 and 2 by the same author in HUMAN POWER vol. 5, no. 2, summer 1986. - Dave Wilson)

## Summary

The progress made in fibre-reinforced composites and the resulting advanced aerodynamical design (laminar-flow airfoils) over the past 15 years has made it possible to build human powered planes with half the previous weight, and of aerodynamically sophisticated design.

Conventional high - wing monoplanes with faired hanging cabin and all - moving rudders have been tested with great success. The German planes MUSCULAIR I and II are to be considered as aerodynamically highly sophisticated as they have no wire bracing and no energy storage. With MUSCULAIR II an average athlete improved on the record speed in the Kremer World Speed Competition with about half the power requirement compared to the rest of the competitors.

The whole range of possible flying speeds were investigated for human-powered planes of optimum design at the present state of technology. A minimum power requirement of under 200 watts is possible with extremely large planes which are very difficult to handle and to fly.

There is an optimum configuration at a flying speed of about 8.5 m/s. This plane with about 25 m wing span has a power requirement slightly below 200 watts (near the ground) with a glide ratio of 44 and can be flown by experienced light-weight pilots.

CYCLAIR can be built at a weight of slightly over 30 kg with the following design characteristics.

- fully sandwich-covered wings with laminar-flow airfoil
- carbon-fibre-reinforced epoxy main spar in four sections designed for three times the static load

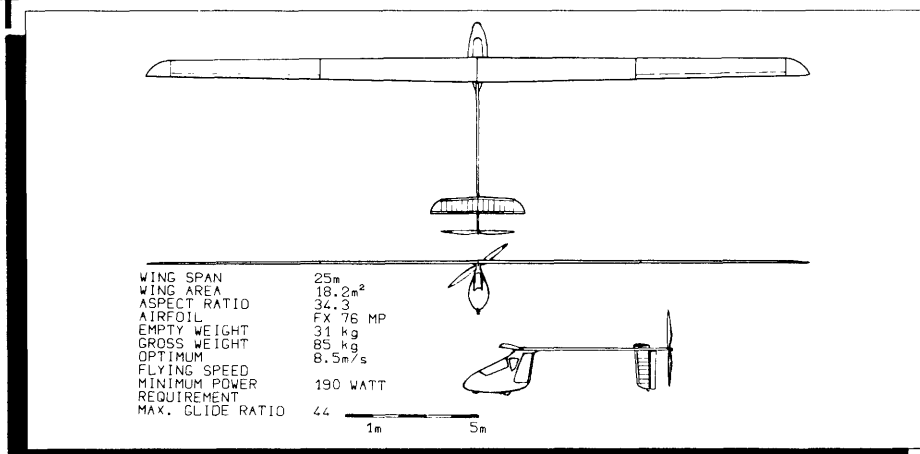


FIG. 1 The cantilevered high-wing monoplane Cyclair combines minimum power demand with good-natured flying behavior.

- sandwich-covered cabin with semi-recumbent pilot position
- all-moving elevator
- all-moving rudder with auxiliary rudder
- rear propeller to protect the plane from avoidable turbulences

This CYCLAIR plane is similar to the MIT- designed MICHELOB LIGHT EAGLE which is larger, a little heavier and optimized for slower flying speed. With this MICHELOB LIGHT EAGLE, MIT will make the flight legend of Daedalus a reality in the near future.

This 110-km-long flight from Crete to the Greek mainland will be the climax and perhaps the end of the initial phase of human-powered flight which will remain a privilege for few enthusiasts only because it requires both a high-grade technology and a high-level of effort of the pilot.

The prizes donated by Henry Kremer were worldwide a great incentive for the development of many human-powered aircraft. The precise design of high-strength ultralight construction is also necessary for planes with the lowest possible power requirement like electric or solar-powered planes or unmanned high-altitude crafts for communication relays in the stratosphere.

## General

Bryan Allen was the first who completed the one mile long, figure-eight flight with Paul MacCready's GOSSAMER CONDOR in 1977, and

crossed the English Channel in 1979 with the GOSSAMER ALBATROSS, setting two incomparable milestones in the history of aviation.

The Kremer World Speed Competition demanded a flight over a 1500-m-long triangular course to be covered within three minutes and allowed storage of the pilot's energy ten minutes prior take off.

This prize was first won by an MIT student group with their MONARCH in May 1984. Four further prizes have been awarded for flights to improve the existing record by at least five percent. MacCready did this with the Bionic Bat in July and December 1984. Both MIT and MacCready used energy storage.

Also in 1984, a German amateur team, unsupported by any large wealthy sponsor, built their first human-powered aircraft, MUSCULAIR 1. Two weeks after completing the MUSCULAIR 1 they won the figure-eight Kremer prize for non-Americans with a speed almost twice as fast as MacCready's GOSSAMER CONDOR. Two months later they won the Kremer speed prize in August, 1984 by improving MacCready's speed of the BIONIC BAT by seven percent, without energy storage.

To test the reserves of pilot and aircraft they made the first human-powered passenger flight in the history of aviation on October 1, 1984.

In 1985 this airplane was involved in a traffic accident on the road and was heavily damaged. The team decided to build the MUSCULAIR 2, being an aircraft designed for high speed. Again

they won the Kremer speed prize and improved their world record from 35.7 km/h to 44.3 km/h.

To get an impression of the size and weight of the airplanes:

MUSCULAIR1: span 22 m;  
empty weight 28 kg  
MUSCULAIR 2: span 19.5 m;  
empty weight 25 kg

This paper deals mainly with experiences gained by the MUSCULAIR projects and with possible developments corresponding to the present state of the art as well.

### General considerations of plane conceptions

Although many pioneers achieved their great successes with canard-type planes (Wright brothers, Focke, MacCready and the latest, Burt Rutan and Jeana Yeager with their Voyager in Dec. 1986) this conception could, despite its stall safety, not represent a breakthrough.

The following four disadvantages are mainly responsible:

- the unavoidable side-faces of the fuselage located far in front of the center of gravity make yaw control difficult. Sometimes a power-consuming swept-back main-wing design is necessary;
- the lift of the canard wing is generated with too much induced drag because of its low aspect ratio;
- the main wing often does not operate at the best glide ratio or minimum sinking velocity, as its angle of attack cannot be adjusted as can that of the canard wing; and
- the canard wing affects the field of vision.

Conventional high-wing monoplanes with faired hanging cabins and all-moving rudders have proven to be the best for light-weight, efficient, safe and simple controllable HPAs.

With the increased knowledge of the precise design of high-strength micro-light construction, designers will turn to cantilevered structures that eliminate external wires. Rough estimations at the early design state of MUSCULAIR 1 clearly showed that the power demanded due to the increase of structural weight is more than outweighed by the lower drag of a cantilevered design. The contribution of ground effect from the use of low-winged monoplanes was generally overestimated.

Spring-neutralized all-moving elevators and rudders turned out to be both light-weight and effective. Based on the analyses of test flights the author thinks that an all-moving rudder with an auxiliary rudder is more favorable.

Front, middle and rear propeller positions have proven equivalent in successful HPAs, although the middle and rear-arrangements are aerodynamically better.

A favorable aircraft concept combining minimum power demand and good-natured flying behavior is the cantilevered high-wing monoplane CY-CLAIR (*Fig. 1*) with laminar-flow airfoils, hanging faired cabin with the pilot in a semirecumbent position, all-moving elevator, all-moving rudder with auxiliary rudder and pusher propeller.

The design considerations of this new design will now be discussed.

### Optimization from long-distance flight to high-speed flight

Based on the just-mentioned considerations and on the aircraft weights that can be reached with advanced aerodynamic microlight design, the whole range of human-powered flight was investigated from long-distance flight with minimum power requirement to short-time higher-speed flights.

Only the best laminar-flow airfoils in the range of Reynolds numbers from 300,000 to 800,000 were considered, such as the FX 76 MP, designed in 1976 by Prof. F. X. Wortmann especially for HPAs.

The following main influences were taken into consideration in making the optimizations:

- aircraft dimensions and corresponding weights;
- ground-effect factor of 0.8 (flying altitude about 1/4 wing span);
- lift coefficient not over 1.1 in order to have enough stability and control reserves;
- Reynolds numbers not below 300,000 to avoid unexpected laminar-bubble separation with hysteresis effects; and
- minimum chord length at the wing of a low-speed long-distance plane, 0.7 m; a high-speed plane, 0.4 m

*Figure 2* shows the rapid decrease in wing area with increasing flying speed.

The optimum wing span and chord length of a trapezoid wing with the corresponding sinking velocity and power requirement is given in *figure 3* for the whole flying-speed range.

The most important results of the optimization are shown in the velocity polars (*fig. 4*). The minimum power requirement of HPA at the present state of the art is slightly more than 150 watts (near the ground), achievable with a low-speed plane (about 6 m/s) of over 25-m wing span. The author is of the opinion that wing-spans larger than 25 m are not practical, because this gives nearly no reduction in power requirement, but the aircraft becomes hard to control because of the increased mo-

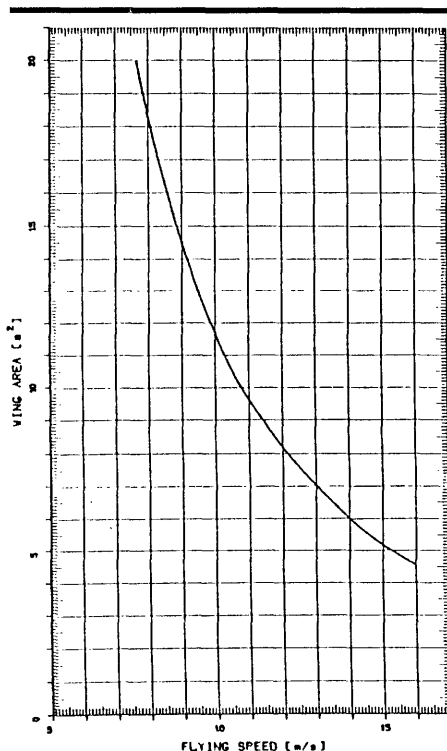


FIG. 2: Wing Area Required for  $CL = 1.1$

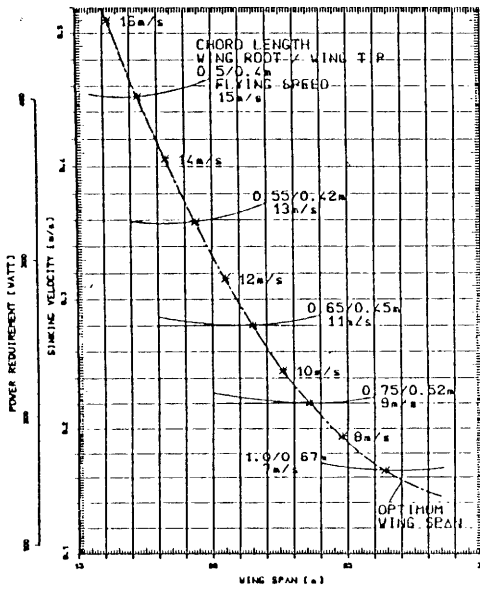


FIG. 3, Min. sinking velocity and power requirement and optimum wing configuration of man-powered planes.

ment of inertia, even with extremely lightweight construction. In addition, aircraft become quite sensitive to gusts.

A favorable wing has 25-m span (18m<sup>2</sup> wing area), has a maximum glide ratio of 44, and a power requirement of only 190 watts. Such a wing can be satisfactorily handled and controlled by an experienced pilot.

This CYCLAIR-type of plane is capable of covering long-distance flights, even against light headwinds, and does not react so sensitively to gusts because of the higher flying speed.

At a flight speed of more than 13 m/s a very high power is required with an airplane with smaller wingspan. The high-speed aircraft MUSCULAIR 2 showed that first-class athletes are capable of maintaining such speeds for a few minutes only. With such an airplane it seems possible to fly the 1500-m speed course in about 100 seconds without energy storage; this means a flight speed of 54 km/h. A new speed record could be set with such an airplane.

**Wing shape and structure**

Though an elliptically shaped wing seems aerodynamically the best, a trapezoid wing is preferred for design and aerodynamical reasons. A trapezoid wing can be built to be simpler, lighter in weight and more accurate in shape, and the airfoil operates better at the wing tips because of the larger chord length and high-

er Reynolds numbers there.

The increase in induced drag near the ground is small when turning away from the ideal elliptical lift distribution. More important are well-shaped and profiled wing tips. With the semicircular design of the wing tips the effective wing span is increased and hence the induced drag is slightly reduced.

To build a light-weight, strong wing that is stiff torsionally and in bending with the necessary accuracy required for laminar-flow airfoils, the application of carbon-fibre-reinforced spar and foam/fiberglass sandwich covering is necessary (fig. 5). For aerodynamic reasons the sandwich has to cover at least the whole laminar area on the upper side and from the nose to the curvature inflection on the lower side. In order to get the wing torsionally stiff enough the nose covering and the spar should form a closed tube. However, the sandwich covering and the carbon spar deform differently under load. On the wings of the MUSCULAIR 2 boundary-layer transition occurred too early just behind the spar on the upper side. This can be avoided with a slightly flexible skin covering the spar.

The best solution seems to be a wing-structure as shown in Fig. 5 with a flexible aileron connection forming an integral part. These flexible connections have been tested successfully in gliders (Speed Astir) and model aircraft.

**Elevator and rudder**

All-moving elevators and rudders, applied mainly for weight reasons, have generally proved to be good. An all-moving vertical tailplane with auxiliary rudder seems to be better for lateral control. Airfoils with 9-10 percent thickness, like the NACA 0009 or the FX100 MP, are favorable as they work well even at low Reynolds numbers (below 300,000). Although elliptical tail wings are aerodynamically better the trapezoid shape is advantageous as it can be built easier and lighter.

When arranging the elevator, great care has to be taken that it avoids the downwash turbulence of the wing at all flight altitudes.

**Fuselage**

It was found that the pilot delivers about the same power output in semi-recumbent position as in the upright position. In the semi-recumbent position the cabin can be made smaller. The aerodynamic drag can be further reduced through the use of an extremely light fiberglass sandwich fairing at least in the front part which ensures a more accurate shape and surface finish.

The supporting fuselage structure with the wing connections and the stabilizer strut in which the propeller shaft rotates are preferably made of carbon-fibre tubes.

**Drive and propulsion**

Although the flapping wing can in theory be made quite efficient, the propeller is by far the most efficient means of propulsion. A maximum efficiency of 90 percent can be reached in HPA only with relatively large slowly running propellers designed for minimum induced losses. Larrabee's elegant method has to be mentioned here.

A large propeller adds weight and beyond a certain size the tips are likely to strike the ground when the aircraft is taking off or landing. Therefore the diameter required for good efficiency (89 percent) and medium efficiency (85 percent) is given in fig. 6.

The chain drive is highly efficient,

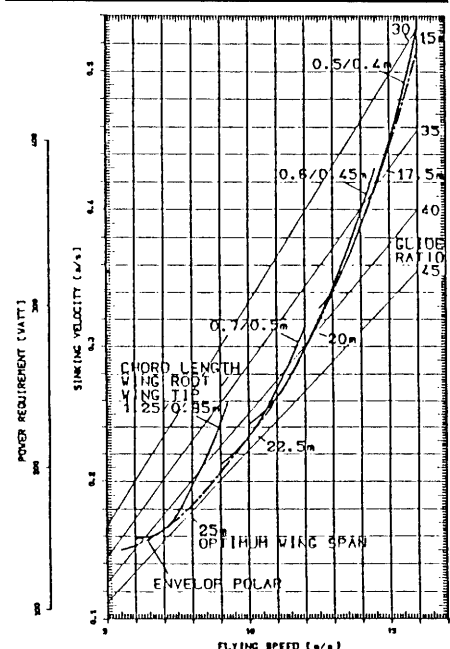


FIG. 4; Velocity polar of man-powered planes with optimum wing configuration

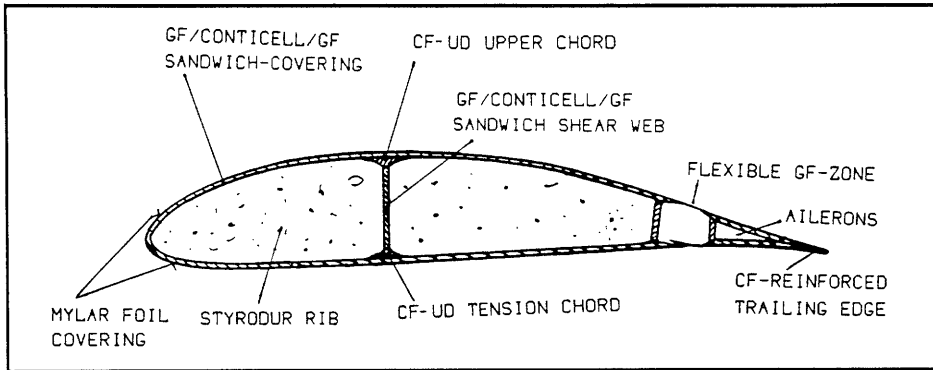


FIG. 5: Wing structure with Wortmann Airfoil FX 76 MP 160

light-weight and reliable when carefully designed and built. In HPA-projects in Japan and Germany it was found that the pedal-power output could be improved by about 5 percent through the use of an elliptical chainwheel.

In order to protect fuselage and wings from the accelerated and turbulent slipstream of the propeller, it was often located behind the wings (MacCready's BIONIC BAT) or behind the tail plane. (Rochelt's MUSCULAIR 1 and 2).

Although a long propeller shaft is necessary a pusher propeller is advantageous, as the tail plane works more effectively in the accelerated air flow before a propeller, and the power demand of the HPA can be slightly reduced.

**Controls**

Most HPA designers have arrived at elegant andergonomic control. Because precise control with steering handlebars (fig. 7 shows the MIT-design) is very important, the pilot must keep his/her body almost immobile above the hips to allow the controls to be handled sensitively, while cycling with high power output.

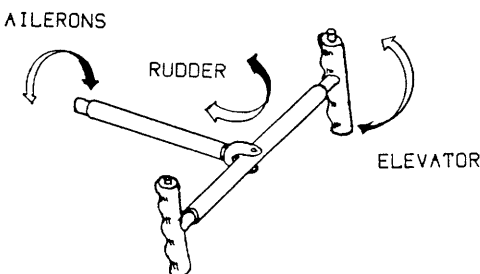


FIG. 7: Three-axis control stick.

When steering, the pilot has only to imagine that he holds the wingtips with his hands and moving the controls will cause the plane to perform the desired maneuvers.

Sideway tilting of the control bar operates theailerons, rotation around the vertical axis acts upon the main rudder, and tilting the handgrips around the horizontal axis acts on the elevator. As the aerodynamic control forces are rather small, it is practical to install self-centering spring units.

For long-distance flights it is desirable to install an automatic control system to reduce the pilot's mental workload. Such an autopilot can improve the system performance by maintaining flight near minimum power requirement.

For the Daedalus project MIT designed an autopilot that weighs only a few hundred grams, so that the pilot can concentrate more on power performance and navigation.

**Technological outlook**

MIT may be making the flight legend of Daedalus a reality in the near future. This may be the culmination of human-powered flight which will remain a privilege to a few enthusiasts and universities only, because it requires both a highly sophisticated technology and high athletic and flying effort of the pilot.

The development of human-powered helicopters is, because of the high power requirements and the stability and control problems, very difficult.

Nevertheless, Professor Akira Naito's team from Nihon University Tokyo did in fact succeed in getting their helicopter

A DAY FLY a few centimeters off the ground for a few seconds on Dec. 6, 1985. As the power requirement for getting out of ground effect is more than 2 kilowatts, it does not seem to be likely that a general break-through will be achieved in the near future.

The precise design of high-strength microflight construction developed for HPA in the past years spurred work in the unusual aerodynamics at Reynolds numbers between those for model aircraft and there for gliders.

The technology developed will also benefit the unmanned high-altitude aircraft powered with solar orhybrid energy, used for example for communication relays which can remain aloft in the stratosphere for weeks or months.

E. Schoberl Ossiacher Str. 42  
D8500 Nurnberg 50  
West Germany

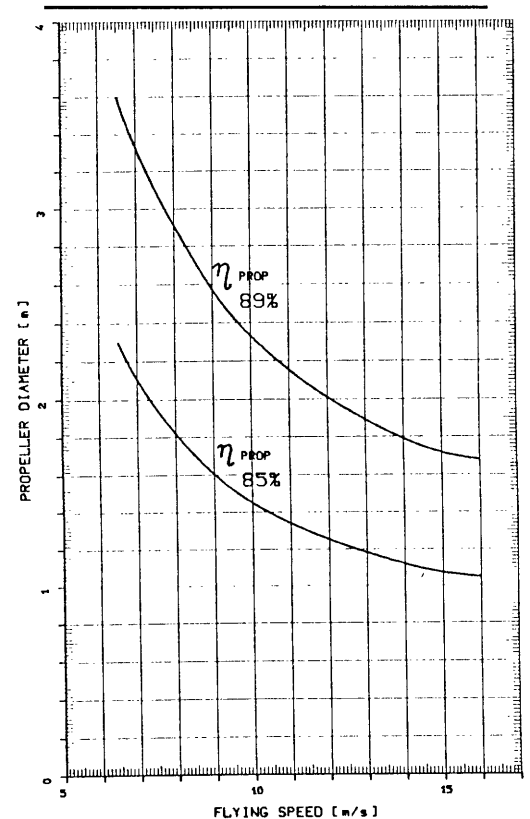


FIG. 6: Propeller diameter required for 85% and 89% efficiency.



continued from front page

Many, if not all, of the new high-speed craft will be hydrofoils. By literally flying through the water, hydrofoils eliminate the water drag of a hull. The required wing area for a fast hydrofoil is quite small – on the order of .5 square feet or less. This paper will discuss the design of human-powered hydrofoils, concentrating on wing sizing based on power available, minimum flight power, takeoff speed, and structural considerations.

There are many hydrofoil configurations suitable for human-powered applications. Here I will concentrate on the Flying Fish configuration (Figure 1) – a single main wing under the center of gravity and a small forward stabilizer wing which carries little or no load. The main wing is supported at its center by a single strut which houses the drive mechanism to the propeller. Other more complex configurations (ladder foils, biplanes, multiple support struts, etc.) may prove to be better for really fast designs. The analysis ideas presented here can be readily extended to these cases.

### Hydrofoil History

Brad Brewster [1] designed a human-powered hydrofoil as a bachelor's thesis project at MIT, but did not pursue development because the V-foil configuration was predicted to have only moderate performance. He concluded that tandem fully-submerged foils were the best approach, but stability and control of this configuration would be a very complex problem. Jon Knapp experimented with hydrofoils on early versions of his Sea Saber, but never was able to get the hull completely out of the water, and concluded that the craft with hydrofoils had more drag than without hydrofoils.

James Grogono, a hydrofoil sailing enthusiast in England, developed the first human-powered hydrofoil craft to successfully 'fly' on its foils [2] – a rowing shell equipped with a central fully-submerged foil, and a V-foil in front – but it too had more drag with foils than without. David Owens, also in England, has been developing Foiled Again, a kayak outfitted with hydrofoils and propeller drive, for the last few years [3], with moderate success.

The author and Allan Abbott have recently developed the Flying Fish and Flying Fish II hydrofoils [4,5]. The configurations of the Flying Fishes are quite different from previous designs. They incorporate tandem submerged foils, active depth control, and a standard cycling position. The original Flying Fish, powered by Steve Hegg, now holds the flying-start 2000-m record with a time of 6:38 (the standing-start rowing record is 6:49).

### Hydrofoil Drag, Propulsion, and Performance

#### Hydrofoils vs. Airplanes

A hydrofoil is essentially the same as an airplane, but with the wings in the water. Water is more than 800 times more dense than air so we might expect larger drag. However, since lift and drag are both proportional to density, the overall drag of a hydrofoil wing should be no higher than for an airplane wing. The hydrofoil wing has 800 times as much drag per unit of area, but it needs only 1/800<sup>th</sup> the area of the airplane wing.

A very simple estimate of the speed attainable can be made based on the propeller and drive-train efficiency,  $\eta$ , the power-to-weight ratio,  $P/W$ , and the lift-to-drag ratio,  $L/D$ :

$$V = \eta P/W L/D$$

Assuming an efficiency of 80% (.8), power of 0.5 HP (550 ft-lb/sec) weight of 200 lb. and  $L/D$  of 40, the predicted speed is 44 ft/s, or 26 knots. These are approximately the values for the Rochelt Muscalair II human-powered airplane. The  $L/D$  of 40 is typical of a modern sailplane ( $L/D$  is equivalent to the glide ratio), but is extremely good for a human-powered airplane. Hydrofoils have sources of drag related to the air-water interface that airplanes do not have, and hence have lower  $L/D$  values than airplanes. These differences will be explained in greater detail below.

Even if a hydrofoil  $L/D$  of only 20 could be achieved, 13 knots would be possible on 0.5 HP, and 26 knots on 1.0 HP. It should be noted that for a given hydrofoil craft, the  $L/D$  is a function of speed, and decreases with increasing speed above a certain speed. It is also more difficult to make a hydrofoil with  $L/D$  of 20 at 26 knots than at 13 knots. While it is true that a wing alone optimized for 26 knots can have the same  $L/D$  as a wing optimized for 13 knots, the drag of the rider and framework in the air is higher at 26 knots, resulting in a lower overall  $L/D$ . High-speed hydrofoils can certainly benefit from lightweight aerodynamic fairings similar to those used on land vehicles.

#### Induced and Wave Drag

Like airplanes, hydrofoils have drag as a by-product of producing lift, called induced drag. Hydrofoil-induced drag has the same functional form as airplane-induced drag, but there is an additional multiplicative factor,  $f_i$ , to account for the proximity of the wing to the water surface.

$$D_i = q C_{d_i} S$$

$$= f_i W^2 / (\pi q b^2)$$

$$C_{d_i} = f_i C_L^2 / \pi A$$

$$C_L = W / (q S)$$

$$q = 0.5 \rho V^2$$

Here,  $\rho$  is the density of water,  $V$  is the velocity,  $q$  is the dynamic pressure,  $W$  is the total weight,  $C_{d_i}$  is the induced-drag coefficient,  $C_L$  is the wing-lift coefficient,  $S$  is the wing area,  $b$  is the wingspan, and  $A$  is the aspect ratio ( $\equiv b^2/S$ ).

Hoerner [6] gives more information on the factor  $f_i$ . If the wing is far below the water surface,  $f_i$  is equal to one, giving the same induced drag as an airplane. As the wing approaches the surface, a sort of 'reverse ground effect' occurs, increasing induced drag because the wing has less fluid available to act upon. When the wing is at the surface, the fluid volume around the wing is halved, and  $f_i$  reaches a limiting value of 2.

Unlike airplanes, hydrofoils can produce waves which cause an additional drag component, although experience with the Flying Fish suggests that wave drag is very small. Except at very low speeds, near stalling, the visible waves from the Flying Fish are very small. Hoerner [6] also reports that shallow water can reduce or eliminate wave drag. In fact, wave drag vanishes at a critical speed,  $V = (g H)^{.5}$ , where  $g$  is the acceleration of gravity and  $H$  is the water depth. At a typical hydrofoil speed of 12 kt (20.2 ft/s) the depth required is 12 ft. At much lower depth, wave drag is probably still negligible, and the induced drag may be decreased due to ground effect as the wing nears the bottom.

Profile Drag

Profile drag is the drag of the wing and strut sections, and is of the same form as that for airplanes:

$$D_p = q C_{d0} S$$

where  $C_{d0}$  is the profile drag coefficient.  $S$  is the reference area (usually span x average chord).

Selection of the proper foil section is critically important to achieving optimum performance. Circular-arc foil sections as used on large powered hydrofoils are not appropriate for human-powered applications. These are designed to minimize the pressure variation on the upper surface, and thus minimize the possibility of cavitation. They do not have particularly low profile drag. Human-powered hydrofoils are slow enough that cavitation is not a concern, so the foil can be a standard airfoil as used on airplanes. For practical hydrofoil designs, it is usually desirable to have a low takeoff speed, hence high  $C_{Lmax}$ , and low drag at high speed, hence low  $C_{d0}$  at low values of  $C_L$ . These requirements are the same as those for sailplanes, which must circle slowly in thermals, and fly at high speed between thermals.

The Reynolds numbers for hydrofoils (200,000 to 1 million) are too low to make use of full-scale sailplane airfoils. (Reynolds number: a measure of the ratio of inertial forces to viscous forces:  $Re \equiv V c \rho / \mu$ , where  $c$  is the wing-chord length, and  $\mu$  is the viscosity). Luckily, these Reynolds numbers are a good match to those of radio-controlled model sailplanes. Especially applicable is the F3B competition category, in which one of the events is a high-speed run. F3B competition has become increasingly fierce in recent years, and considerable analytical and experimental effort has gone into airfoil design. The HQ airfoil family, designed by Quabeck [7,8], appears to have the best overall performance. These are a family of airfoils of differing thickness and camber.

Airfoil profile drag coefficients generally decrease with increasing Reynolds number. For model airfoils between Reynolds numbers of 200,000 and 600,000, the drag coefficient varies approximately as  $R^{-.35}$ . Obviously, performance will be better if, all other things being equal, Reynolds number is increased. A property of water is that its viscosity decreases with increasing temperature. Thus Reynolds number, and hence drag, can be minimized by operating in warm water. The drag reduction is modest, but

could be enough to make a significant difference in record trials. The following table illustrates this phenomenon for a 3-inch chord section at 12 kt.

Temp (deg F)	$\mu/\rho$ ft <sup>2</sup> /sec ( x 10 <sup>-5</sup> )	Re	section drag relative to 70 deg
50	1.41	359,000	1.10
60	1.22	415,000	1.05
70	1.06	477,000	1.00
80	.93	544,000	0.96
90	.83	610,000	0.92

A rule of thumb is that the profile drag coefficient decreases one percent for every 2 deg F increase in water temperature. For simplicity, Reynolds-number effects will not be included in the examples below. If Reynolds-number effects were included, the optimum spans and aspect ratios would be slightly smaller (i.e. larger chord), driven by the decrease in profile-drag coefficient with increasing chord.

Interference Drag

Interference drag is caused by the mutual interference of wings and struts at an intersection. There is no easy way to calculate interference drag. Hoerner [6] presents some estimation techniques, based on various test data. For a basic "T" intersection of two foil sections, Hoerner gives the following:

$$D_{int} = q C_{d_{int}} t^2$$

$$C_{d_{int}} = 17 (t/c)^2 - 0.05$$

where  $t$  is the average thickness of the intersecting struts, and  $t/c$  is the average thickness-to-chord ratio. This formula is only a rough guideline. Addition of good filleting, or staggering of the intersecting foils in a streamwise direction, can greatly reduce or eliminate interference drag. A practical solution for a human-powered hydrofoil is to cantilever the wing forward from the vertical strut.

Spray Drag

The vertical struts which support the hydrofoils create a spray of water at the point where they pierce the water surface. It might be expected that spray could be reduced if the strut section has low  $t/c$  and a sharp leading edge. However, experience with a variety of strut shapes for the Flying Fish showed that the amount of spray is largely independent of the leading edge shape. Hoerner's [6] discussion of spray drag indicates that it is only a function of the thickness of the strut:

$$D_{spray} = .24 q t^2$$

Thus the spray drag is roughly equal to the drag of a  $t/2$ -by- $t/2$  flat plate aligned perpendicular to the flow. On the Flying Fish, the spray originates at the leading edge of the strut, and climbs about 8 inches up the side of the strut as a sheet as it goes back. The added 'wetted area' of the strut results in additional skin-friction drag.

Air Drag

It is usually not necessary to consider air drag on a human-powered water craft, as the speeds are quite low. But in going for all-out speed, say 20 knots, air drag becomes quite significant, so aerodynamic streamlining should be added. Drawing on the analogy of hydrofoils and airplanes, a hydrofoil without aerodynamic streamlining is akin to a human-powered airplane without fuselage streamlining. Of course, aerodynamic streamlining on watercraft has many practical problems, foremost of which is safety. Watercraft, especially hydrofoils, can and do capsize. A rider inside a streamlined enclosure may find it very difficult to escape while submerged. Partial streamlining such as handlebar fairings, streamlined tubing, and special clothing is much more practical.

Propulsion

Virtually all of the new generation of high-speed water vehicles will be driven by propellers. It has been known for a long time that propellers are more efficient than oars (albeit less practical in weedy lakes or shallow water). Efficient propellers for human-powered craft are quite different from propellers used on engine-powered boats. Slender blades and steep pitch are the rule for human-powered applications. One of the first applications of such propellers was on Calvin Gongwer's human-powered submarines in the mid-1950's. More recently, propellers optimized using the methods of Larabee [9] are used on craft such as the Knapp Sea Saber, the Owers Foiled Again, and the Brooks/Abbott Flying Fish series.

It is possible to get propulsion directly from a hydrofoil wing if it is flapped up and down. This approach has high efficiency theoretically, but is quite difficult to implement. The first known flapping hydrofoil craft is seen briefly in the movie "Gizmo!". It consisted of two hydrofoil wings, one for each foot, with handholds to aid in pitch control. The 'rider' stands sideways to the direction of flight and flaps the wings with arm and leg motions. Nothing is known about the designer or origin of this craft. Bill Watson recently made a reproduction [10], but it proved to be impossible to control. Parker MacCready, an engineering-science graduate student at Caltech, is now researching flapping hydrofoils [11]. He recently completed a testbed flapping-wing vehicle with a configuration similar to that of the Flying Fish.

Hydrofoil Design Considerations

In this section, the functional relationships of the various design parameters will be given. Recall that the designs in this paper will be based on the Flying Fish configuration. The goal of the design process will be to select the optimum wingspan and aspect ratio, based on several design criteria. The main criteria are: speed at design power, minimum power, takeoff speed, allowable bending stress, and wing-tip deflection. In order to easily see how these factors interrelate, graphs will be given where constant values of the factors (contours) are plotted on axes of aspect ratio and span. By overlaying these plots, insight can be gained into various tradeoffs (e.g. how much can speed be increased by going from a fiberglass wing to a carbon-fiber wing?).

The following table lists the values of the variables used in creating the graphs in the following sections.

symbol	description	value	units
$\rho$	density of water	1.938	slugs/cu-ft
$\rho_{\text{air}}$	density of air	0.00238	slugs/cu-ft
$C_{L\text{max}}$	max wing lift coef.	1.1	
$W$	weight	190	lb.
$t/c$	thickness ratio	.13	
$\lambda$	taper ratio	.4	
$\eta_{\text{prop}}$	propeller efficiency	.85	
$f_i$	ind. drag factor	1.48	
$C_{d_o}$	wing profile drag	0.008	
$C_{d_{\text{strut}}}$	strut profile drag	0.0085	
$S_{\text{strut}}$	strut area	0.46	ft <sup>2</sup>
$C_{d_{\text{fw}}}$	front-wing drag	0.009	
$S_{\text{fw}}$	front-wing area	0.43	ft <sup>2</sup>
$C_{d_{\text{spray}}}$	spray-drag coeff.	.24	
$t_{\text{strut}}$	strut thickness	.0917	ft
$C_{d_{\text{air}}}$	air-drag coeff.	.7	
$S_{\text{air}}$	frontal area in air	7	ft <sup>2</sup>

Design Power

The starting point for design of a human-powered hydrofoil is the design power level. It is determined from the duration of race or event for which the hydrofoil should be optimized. Of course the duration of a distance event depends on the expected speed – some guesswork or iteration is required in these cases. There are published curves ( see e.g. Whitt and Wilson [12] ) which show the attainable power output of various types of humans (from average people to world-class athletes) for different durations of exercise. For the design examples in the next section, the following three combinations of power and duration will be used:

Duration	Power	Application
40 seconds	1.0 HP	200-m event
6 minutes	0.5 HP	2000-m event
1hr	0.25 HP	recreation

Maximum Speed

The maximum speed occurs when the design power, reduced by the propeller efficiency, is equal to the power required. The power required is the product of the velocity and the sum of all of the drag components. For simplicity, all of the drag terms which are not related to the wing are summed to give an equivalent 'drag area',  $S_{\text{ref}}$ . (The air drag term is multiplied by the air-to-water density ratio before summing). The value of  $S_{\text{ref}}$  based on the data in the above table is .0158 ft<sup>2</sup>.

$$P_{\text{des}} \eta_{\text{prop}} = V \{ q C_{d_o} S + q S_{\text{ref}} + f_i W^2 / (\pi q b^2) \}$$

$$= .5 \rho V^3 (C_{d_o} b^2 / A + S_{\text{ref}}) + f_i W^2 / (.5 \pi \rho V b^2)$$

Minimum Power

A hydrofoil optimized for maximum speed at a given power may have quite high minimum power required just to fly. This may be acceptable for an all-out racing machine, but for versatility or recreational use, it may be desirable to be able to fly at a lower power. Specification of minimum power as well as design power places a constraint on the allowable designs, and usually will result in a penalty in speed at the design power.

Minimum power is found by setting the derivative (with respect to velocity) of the power equation equal to zero. This leads to:

$$3 \{ .5\rho V^2 (C_{d_o} b^2/A + S_{ref}) \} = f_i W^2 / (.5\pi\rho V^2 b^2)$$

which can be solved for V, and then V substituted into the original power equation to get the minimum power level. Figure 2 shows contours of minimum power from .15 HP to .35 HP. (The contours were calculated by iteratively calculating values of A that resulted in minimum powers that matched the contour levels).

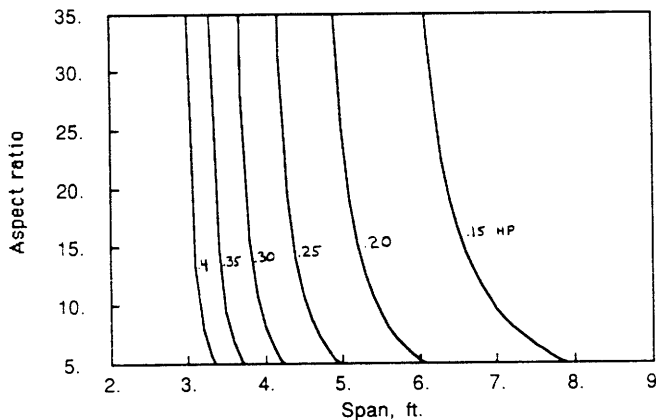


Figure 2. Contours of minimum power required to stay foilborne as a function of wingspan and aspect ratio.

Takeoff speed

Like the minimum power case above, hydrofoils optimized only for speed at high power may prove to have an uncomfortably high takeoff speed. Takeoff occurs when the wing generates lift equal to the total weight:

$$W = C_{Lmax} .5\rho V^2 S$$

Solving for V:

$$V = \{ 2 W / (\rho S C_{Lmax}) \}^{1/2}$$

$$= \{ 2 A W / (\rho b^2 C_{Lmax}) \}^{1/2}$$

It is seen that the takeoff speed varies as the square-root of the wing loading. With a wing loading of 130 lb/ft<sup>2</sup>, the Flying Fish II is able to take off easily. Assuming a C<sub>Lmax</sub> of 1.1, the corresponding speed is 7 knots. Contours of takeoff speeds between 4 and 12 knots are shown in Figure 3.

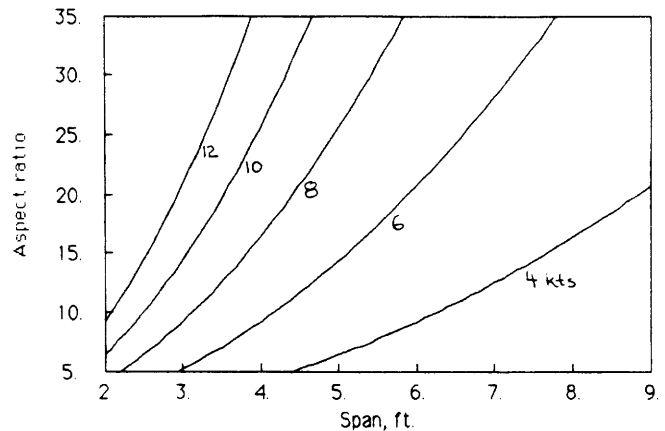


Figure 3. Takeoff speed contours, assuming takeoff at C<sub>L</sub> = 1.1

Bending Stress

The bending stress at the root of a thin high-aspect ratio hydrofoil wing can be very large. (It will be assumed that the hydrofoil wing is constructed as a solid mass of material; no lightweight core, etc). From simple beam theory, the maximum bending stress, σ, is

$$\sigma = M / S_m$$

Where M is the bending moment, and S<sub>m</sub> is the section modulus. Assuming an elliptical distribution of lift along the span, the resultant lift acts 42% of the semi-span out from the root. This leads to a root moment of:

$$M = .11 W b$$

The section modulus is a function of the thickness, chord, and distribution of thickness. For the HQ family of airfoils the section modulus is:

$$S_m = 0.0746 (t/c)^2 c^3$$

The factor .0746 was calculated numerically for the HQ family of airfoils. It doesn't change more than about 10% for other airfoils. After including the effects of wing taper (λ is the ratio of tip chord to root chord):

$$\sigma = .11 W A^3 (1 + \lambda)^3 / \{ 8 * .0746 b^2 (t/c)^2 \}$$

Note that taper ratio and thickness ratio have a strong influence on the root stress. It is especially beneficial to taper

the wing. Although an untapered, constant-chord wing may be easier to make, a tapered wing has much lower stress, and is better hydrodynamically. For an untwisted, straight-tapered wing, a taper ratio of .4 is about optimum for achieving a nearly-elliptical lift distribution. (Twist is not desirable if the wing must operate over a broad range of lift coefficients). A thickness ratio of 13 percent is a reasonable compromise between low drag and structural considerations. Using these values, contours of root bending stress between 5,000 psi and 25,000 psi are shown in Figure 4.

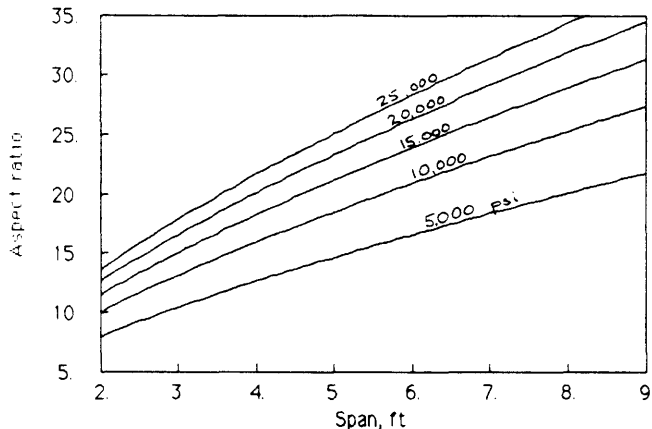


Figure 4. Root bending stress contours, assuming taper ratio of 0.4 and foil thickness/chord of 13%.

Tip Deflection

High-aspect-ratio hydrofoil wings can have considerable deflection at the tip under load. Both translational and torsional deflections are important. If the wing is too flexible, the wingtips may rise up out of the water, or 'flutter' may occur at high speed. Flutter is an aeroelastic (or hydroelastic) oscillation. In airplanes, flutter is often disastrous, tearing the airplane apart. Flutter probably wouldn't structurally harm a human-powered hydrofoil, but it would ruin any chance of going fast, due to a large amount of extra drag. Flutter calculations were not made for either Flying Fish. The wings for both 'Fishes' were designed with a somewhat-arbitrary tip deflection limit of 8 percent of semi-span, i.e. about 3 inches, and flutter has never been a problem.

Torsional deflections alter the spanwise lift distribution, causing increased induced drag. Torsional deflection depends on the torsional stiffness of the wing, sweep angle, the airfoil pitching moment, speed, and location of the shear center of the wing structure. Torsional deflections are beyond the scope of this paper. It suffices to say that torsional deflections should be kept very small.

The normalized tip deflection,  $\Delta = \delta/(b/2)$  can be calculated using elementary beam theory. The result is:

$$\Delta = \delta/(b/2) = f(\lambda, \text{loading}) W A^4 / (64 \cdot .037 E (t/c)^3 b^2)$$

where E is the modulus of elasticity of the wing material. The factor .037 is constant in the wing moment of inertia:  $I = .037 (t/c)^3 c^4$  and is accurate for the HQ family of sections and is reasonably close for other airfoils. The function f, of taper and load distribution, is best calculated by numerical integration of the bending equations. Figure 5 shows contours of tip deflections between 4 and 20 percent of semi-span. Figure 6 shows the effect of the material stiffness. Lines are shown for wood, fiberglass, aluminum, carbon, steel, and HM carbon (special high-modulus carbon), for equal deflections of 8 percent of semi-span.

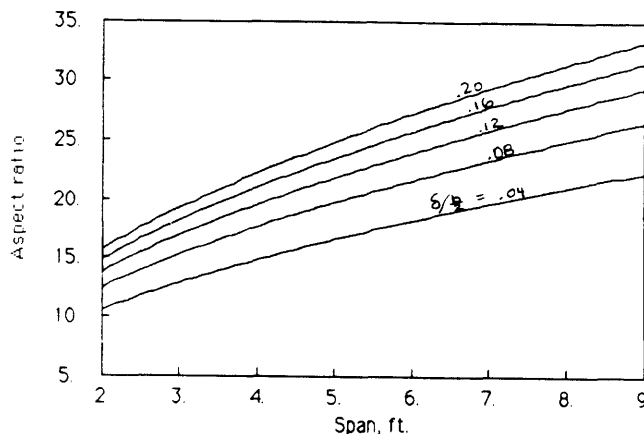


Figure 5. Contours of tip deflection normalized by semi-span (b/2), assuming taper and thickness as in Figure 4, with material properties of aluminum or wet-layup carbon fiber.

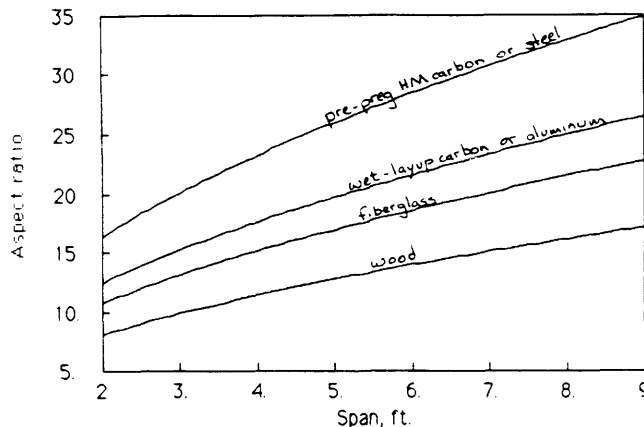


Figure 6. Effect of different wing materials for normalized tip deflection of 0.08.

**Design Examples**

The graphs of the previous section can be used to evaluate the various tradeoffs involved in selecting wing span and aspect ratio. It is not generally necessary to consider stress limits if deflection limits are also applied. The stresses at maximum deflections are almost always quite modest and are well below the ultimate or yield strengths for the material.

Three basic designs will be considered. All will be designed initially to have a minimum power requirement of 0.2 HP to allow extended-duration cruising, and maximum normalized wing deflection of 0.08. The wing construction material is assumed to be either aluminum or carbon fiber/epoxy. The first design is for a recreational craft, with a low design power of .25 HP and maximum takeoff speed of only 4 knots. Second is a competition craft designed for 2000-m races, with design power of 0.5 HP and maximum takeoff speed of 8 knots. Third is a racer for short 200-m sprints, with design power of 1.0 HP and a maximum takeoff speed of 10 knots.

Figure 7 shows contours of maximum speed attainable for the recreational design. Constraint lines for takeoff speed, minimum power, and deflection are also shown. Taken together, the constraint lines form the boundaries of a region, inside of which all constraints are satisfied. The best span and aspect ratio combination inside the region is that which is on the highest maximum-speed contour contained within the region. If necessary, rough interpolation can be used to estimate the shapes of intermediate speed contours. It is seen that the best design point for this case has a maximum speed of about 7.6 knots, with a span of 9 ft and aspect ratio of 20 (the actual optimum is just off the edge of the graph). If the takeoff speed and minimum power constraints are removed, the maximum speed increases to 8.4 knots, the span decreases to 6.5 ft., and the aspect ratio increases slightly to 22. This design still has a relatively modest takeoff speed of about 6 knots (this can be seen by overlaying Figure 3 on Figure 7 or by tracing additional takeoff speed contours onto Figure 7).

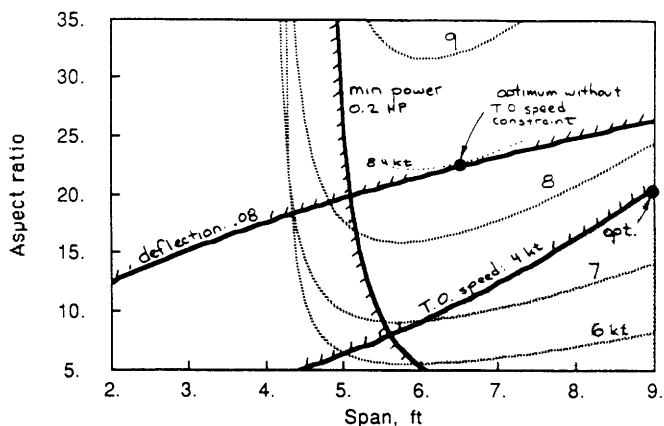


Figure 7. Maximum-speed contours for the recreational (0.25 HP) design, with constraint lines.

Figure 8 shows the results for the long-distance racing craft. The optimum design has a maximum speed of 11.7 knots. In this case, minimum power and deflection are the limiting factors. If the minimum-power and takeoff-speed constraints were removed, the speed would increase only slightly to 11.8 knots (5 min:32 sec for 2000m).

Results for the sprint craft are shown in Figure 9. The optimum design has a maximum speed of 15.3 knots. Without the minimum-power and takeoff-speed constraints, the speed increases to 16.0 knots.

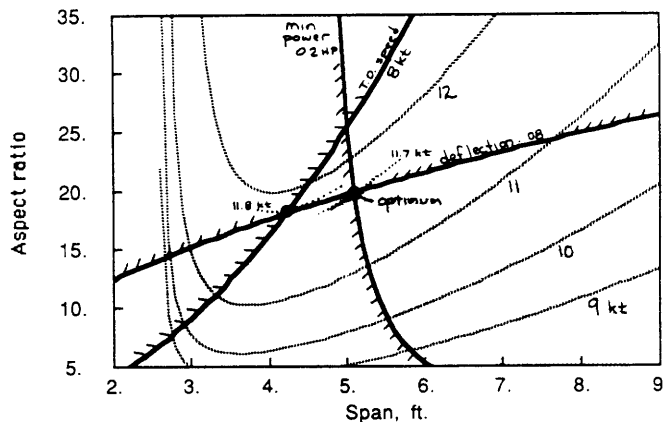


Figure 8. Maximum-speed contours for the 2000-m racer (0.50 HP), with constraint lines.

Figure 10 shows the optimum planforms to scale for each of the three wing designs with the original constraints and without minimum-power and takeoff-speed constraints. The following table gives a summary of the constrained and unconstrained speeds for the three designs.

Design	max speed (knots)	max speed w/o min pwr or takeoff constraints
recreation	7.6	8.4
2000-m	11.7	11.8
200-m	15.3	16.0

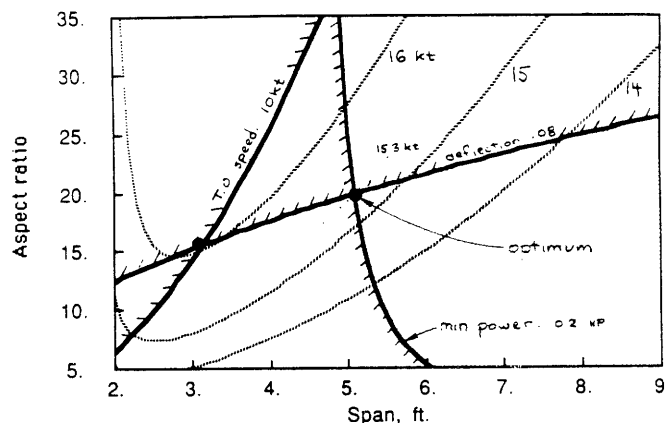


Figure 9. Maximum-speed contours for the 200-m racer (1.00 HP), with constraint lines.

The speed of the best 200-m sprint craft is still below the 20 knots mentioned in the title of this paper. To increase speed further, the wing material could be changed to high-modulus carbon or steel to allow a higher aspect ratio, but this alone isn't enough. The drag of the craft must be reduced as well. With the addition of an enclosed fairing, air drag could be cut in half. The main vertical strut could also be made smaller by about one-half to reduce spray and skin-friction drag. The area of the front wing could be made smaller, also by half. Figure 11 shows the results of these

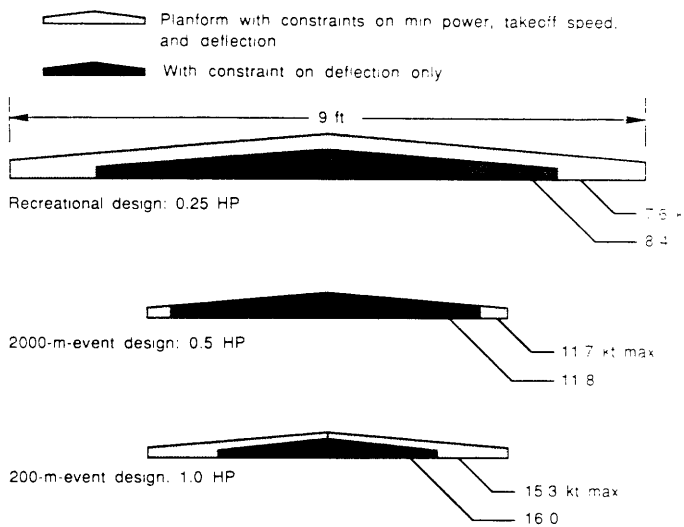


Figure 10. Optimum wing planforms for three optimal designs.

changes along with a deflection-limit line for high-modulus carbon or steel. 20.2 knots can be reached by this ultimate craft with a wingspan of only 2.5 ft and aspect ratio of 18. The takeoff speed of 13 knots may prove to be an inconvenience, however! A larger wing with just 20.0 knots top-speed capability would have a slightly more reasonable takeoff speed of 11 knots.

Figure 12 shows a comparison of the power vs velocity requirements for the three original hydrofoil designs and the final 'ultimate' 20-knot craft. Also shown is the curve for a single rowing shell, based on the data of Rogen [13], and assuming that the efficiency of rowing is 70 percent. Note that at low speeds, displacement hulls are as good as, or better than hydrofoils. It doesn't pay to make a hydrofoil unless you want to go fast and pedal hard!

### Conclusions

The examples in the previous section have just begun to scratch the surface of the kinds of tradeoffs that are possible. Many more questions and tradeoffs can be explored by overlaying the graphs or tracing lines from one graph to another. Questions such as : How much is top speed reduced by having a low takeoff speed? How much faster at 1 HP is a craft optimized for 1 HP than a craft optimized for .25 HP? What is the tradeoff in top speed by setting a low minimum required power? Is it worth the extra money to make the wing out of carbon fiber instead of wood or fiberglass?

### References

1. Brewster, M. B., "The Design and Development of a Man-Powered Hydrofoil," Thesis for Bachelor of Science, Mechanical Engineering Dept, M.I.T., May 1979.
2. Grogono, J. L., "Human-Powered Flight on Hydrofoils: A Successful Sculling-Craft Conversion," *Proceedings of conference on Human Powered Marine Vehicles*, Royal Institution of Naval Architects, London, 1984.
3. Owers, D. J., "Development of a Human-Powered Racing Hydrofoil," *Human Power*, Vol. 3, No. 3, Spring 1985.
4. Brooks, A. N., "The Flying Fish Hydrofoil," *Human Power*, Vol. 3, No. 2, Winter 1984.
5. Brooks, A. N., "Waterbike!," *Bicycle Guide*, Vol. 2, No. 3, May, 1985.
6. Hoerner, S. F., *Fluid Dynamic Drag*, Hoerner Fluid Dynamics, Brick Town, N.J. 1965.
7. Quabeck, H., *HQ profile für F3B, Thermik, Han, Elektro- und Gross-Segler*, Verlag für Technik und Handwerk GmbH, Baden-Baden, 1983.
8. Althaus, D., *Profilpolaren für den Modellflug volumes I and II*, Neckar-Verlag, Villingen-Schwenningen, West Germany, 1985.
9. Larabee, E. E., "Propellers for Human-Powered Vehicles," *Human Power*, Vol. 3, No. 2, Winter 1984.

The 20-knot hydrofoil is certainly a possibility with today's technology. With the encouragement of the IHPVA, and possibly a prize patterned after the Dupont Prize for land vehicles, the 20-knot barrier will surely fall.

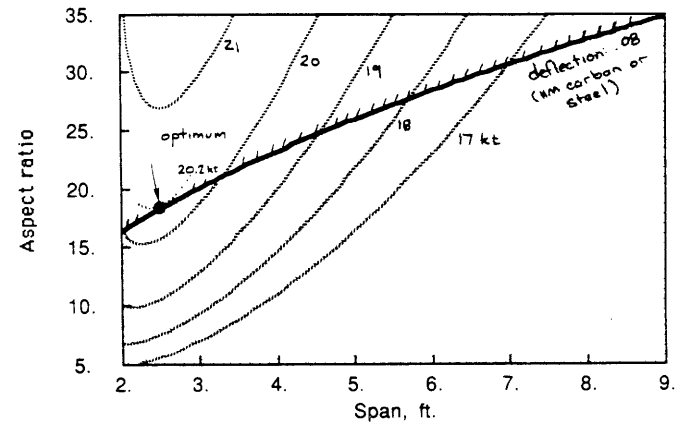


Figure 11. Maximum-speed contours for the ultimate 200-m racer (with reduced air, strut, and front-wing drag), with deflection constraint for high-modulus carbon or steel.

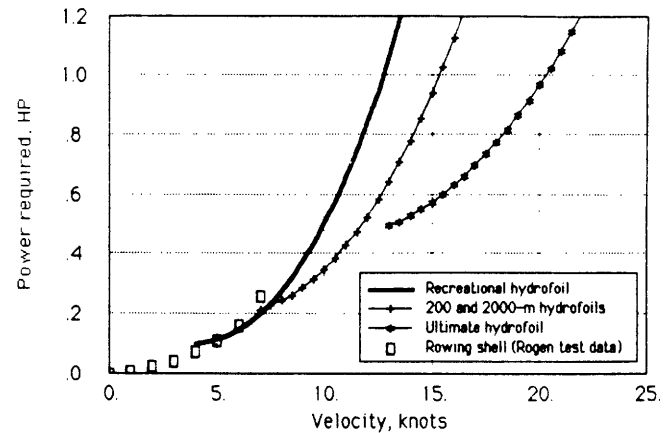


Figure 12. Power vs. speed for the design examples, and for a single rowing shell. Note that 2000-m and 200-m designs are the same due to the minimum-power requirement.

Alec N. Brooks  
1536 N. Altadena Dr.  
Pasadena, California 91107 USA

10. Watson, B., "Current Trends in Water Power," *Proceedings of the First Human-Powered-Vehicle Scientific Symposium*, A. Abbott, ed. IHPVA, Seal Beach, Ca. 1982.
11. MacCready, P., "Features of Flapping-Wing Propulsion," *Proceedings of the Third International Human-Powered-Vehicle Scientific Symposium*, A. Abbott, ed. IHPVA, Seal Beach, Ca. 1986.
12. Whitt, F. R. and Wilson, D. G., *Bicycling Science*, The MIT Press, 1979.
13. Rogen, B., "Determination of Drag Force Relationships and a Drag Coefficient for a Rowing Single Scull," *Proceedings of the Second International Human-Powered-Vehicle Scientific Symposium*, A. Abbott, ed. IHPVA, Seal Beach, Ca. 1982.

# DYNAMICAL STABILITY OF THE BICYCLE

By Y. LeHénaff

*Editor's note: The following paper was sent in by a noted French nuclear physicist. Having had a long series of weighty papers on nuclear physics accepted without demur by various journals, he ventured into the clouded waters of bicycle stability - and had his paper rejected. I created a small storm of controversy when I used some of David Jones' article in PHYSICS TODAY for BICYCLING SCIENCE (I confess I also introduced an error) so that I knew of the lack of agreement in this surprisingly complex field. I wrote to the author to state that HUMAN POWER would be honored to publish his paper, but would invite comment and a rebuttal. Here are all three pieces. - Dave Wilson*

**ABSTRACT**

The first dynamical stability curves for bicycle riding are obtained as solutions of two coupled non-linear equations.

**Introduction**

The theory of bicycle stability has been a long-standing problem since 1898 [1] and culminated with the works of E. Carvallo [2], F. Klein and A. Sommerfeld [3], all using small-angle approximations. The most comprehensive simulation of bicycle riding was done by R. Douglas Roland [4] and involved the computer resolution of eight simultaneous differential equations with more than 70 parameters to describe the "bicycle + rider" system. Using a geometrical approach, D. Jones [5] computed the height of the "fork point" for an infinitely long bicycle, but failed to account for the stability.

The present article solves the problem for a normal-length bicycle with two coupled non-linear equations, derives the first dynamical-stability curves for bicycle riding and analyses the trail effect on steering.

**Gravitation and Centrifugal Forces**

At usual velocities, equilibrium on a bicycle relies essentially on the balance of gravitational and centrifugal forces.

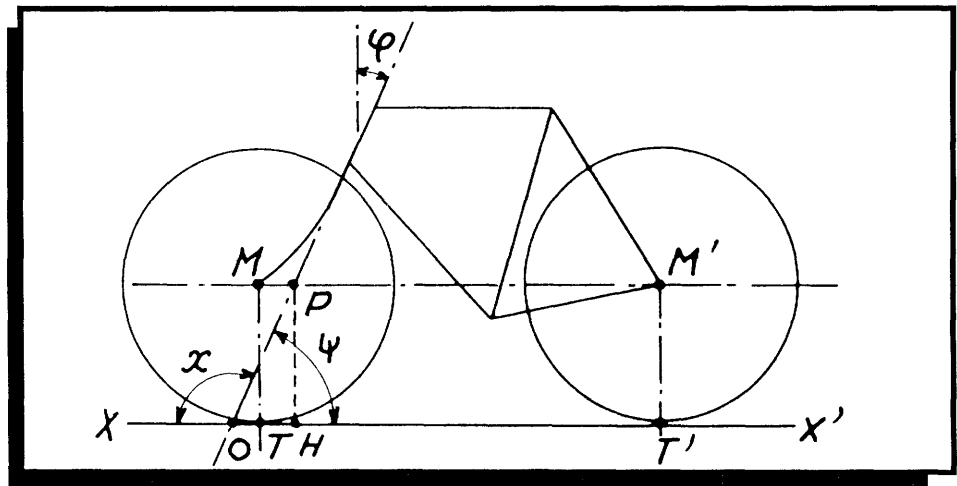


FIGURE 1: Side view and bicycle dimensions. Lengths:  $MM'=TT'=MP + PM' = 1 + L = a = 1.0 \text{ m}$ ;  $l = 0.2 \text{ r}$ ; wheel radii  $r = 0.33 \text{ m}$ . Trail  $T=TO$  is measured positively forwards. The fork angle is  $x = 20^\circ$ .

When the system "rider + bicycle" runs at speed  $v$  on a circular path, the rider leans with the frame tilted by an angle  $\theta$  from the vertical into the curve to offset the centrifugal force. The steering angle  $S$  is the dihedral angle between the plane of the frame and the plane of the front wheel, whereas the angle of turn  $\alpha$  is the intercept of this dihedral angle by the ground plane. If  $a$  is the distance between the wheels' contacts with the ground, the radius of the curve is roughly  $R = a/\tan\alpha$ . With  $g = 9.8 \text{ m/s}^2$ , the system is in dynamical equilibrium when:

$$\tan\theta + v^2 \tan\alpha = (ag). \quad [1]$$

According to tradition, "stability" is meant here by "equilibrium". Other authors [6,7] have analysed steering "stability" to front-fork vibrations that are not considered here.

**Geometry of the bicycle**

For the upright bicycle in Figure 1, the plane of the front wheel coincides with the plane of the frame and cuts the ground plane along  $XX'$ .  $M$  and  $M'$  are the centers of the hubs,  $T$  and  $T'$  the ground-contact points of the wheels. The front fork axis makes an angle  $\varphi$  with the vertical, intercepts the ground at  $O$  and cuts the line  $MM'$  at  $P$ , defined as the fork point.  $P$  is fixed on the fork axis and projects at  $H$  on the ground trace  $OT'$  of the frame plane:  $P$  is also at a fixed position with respect to the center of gravity of the system supposed [4] within

the frame plane. We write  $MP \equiv 1$ ,  $PM' \equiv L$  and, of course,  $1 + L = a$ .

The angles  $\chi \equiv (\text{POX})$  and  $\psi \equiv (\text{POX}')$  are defined respectively in the front-wheel and frame planes; only when those two planes coincide do we have  $\psi + \varphi = \chi - \varphi = \pi/2$ . When the handlebar is turned, it can be seen experimentally that the front wheel slides slightly downwards; therefore,  $\psi$  increases and  $\chi$  decreases.

Jones computed the height  $h$  of the fork point - which is related to the height of the center of gravity and hence to its potential energy -  $h = HP$ , in the frame plane for obvious dynamical reasons. Writing  $OP \equiv \chi$ , we have:

$$h = \chi \sin\psi \quad (2)$$

In the frame plane, the vector relation  $\vec{OP} + \vec{PM}' + \vec{M}'T' + \vec{T}'O = \vec{0}$  projected on  $M'T'$  yields:

$$\chi \sin\psi + L \sin(\psi + \varphi - \pi/2) = r, \quad (3)$$

where  $r$  is the radius of the wheel and  $(\psi + \varphi - \pi/2)$  is the downward tilt of the frame in its plane.

Similarly, in the front wheel plane, the corresponding relation  $\vec{OP} + \vec{PM} + \vec{TO} = \vec{0}$  projected on  $MT$  gives:

$$x \sin(\pi - \chi) + 1 \sin(\chi - \varphi - \pi/2) = r. \quad (4)$$

( $\psi$  and  $\chi$  vary with the angle of turn.)

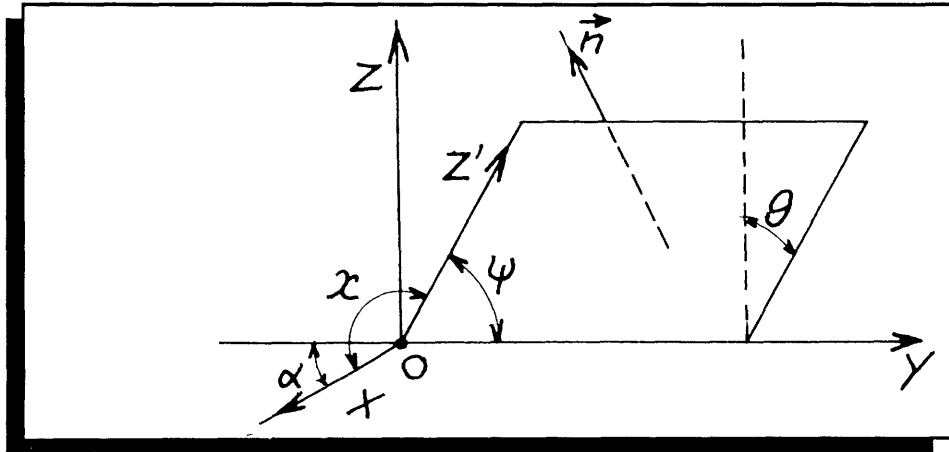


FIG. 2 Schematic diagram of bicycle on a left turn. OX is the ground trace of the front wheel plane and OY that of the frame plane, which is tilted from the vertical plane (OY, OZ) by an angle  $\theta$ . The front-fork axis is along OZ'.

Eliminating  $\chi$  from (3) and (4) provides the first relation between the unknown angles  $\psi$  and  $\chi$ :

$$\frac{r + L \cos\psi \cos\phi}{\sin\psi} - \frac{r + l \cos\chi \cos\phi}{\sin\chi} - a \sin\phi = 0$$

A second relation can be obtained considering a bike running on a curved path (Figure 2). We take 0 as the origin of the coordinates; OZ' as along the fork axis;  $\hat{i}, \hat{j}, \hat{k}, \hat{k}'$  as unit vectors on axes OX, OY, OZ and OZ' respectively; and finally  $\hat{n}$  as the unit vector normal to the plane of the frame.

We have:  $\sin\theta = \hat{n} \cdot \hat{k}$ ,  $\hat{k}' \times \hat{j} = \hat{n} \sin\psi$ ,  
 $\hat{i} \times \hat{j} = \hat{k} \sin\alpha$ ; giving:

giving:

$$\cos\chi + \cos\alpha \cos\psi - \sin\theta \sin\alpha \sin\psi = 0 \quad (6)$$

Eliminating  $\chi$  and  $\psi$  from the coupled equations (5) and (6) provides the relation we need between known quantities ( $r, l, L, \phi$ ) and given ones ( $\alpha, \theta$ ). Algebra leads to an intractable 8th-degree equation, but it can readily be solved by iteration using a small computer.

Figure 3 shows, for various lean angles  $\theta$ , the relative height  $h/r$  of the fork point in the frame plane plotted versus the dihedral angle  $S$  defined previously. The curves also represent - ignoring constant factors - the potential energy of the system. comparison is made with the results of Jones (broken line in Figure 3), using his conventions and bike ( $\phi = 20^\circ$ ,  $l = 0.2 r$ ). The results coincide exactly for  $\theta = 0$  but do depart as the lean increases. Running the program again with a rear wheel 500 meters away does not change the results significantly (circle symbols in Figure 3), and shows

that Jones's solution with the rear wheel set to infinity was fairly good. The remaining discrepancy is now accounted for by an error in Jones's calculation [private communication].

However that may be, maximum stability occurs at absurdly large angles, as already noticed by Jones. We know the moving bicycle to be quite stable when

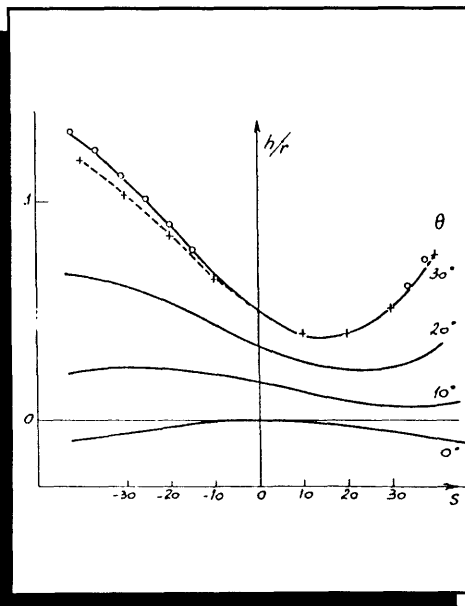


FIG. 3: Geometrical-stability curves Geometrical-stability curves for the bicycle of Figure 1 are shown at different lean angles  $\theta$  in degrees. The height  $h/r$  of the fork point, in wheel-radius units, is plotted versus the steering angle  $S$  in degrees. For clarity, all curves have been arbitrarily shifted vertically. Jones's results for  $30^\circ$  lean are shown in broken line. Circles represent the values obtained with the rear wheel moved 500 meters to the rear.

skillfully ridden, so that a realistic potential curve should display a maximum characteristic of stable motion equilibrium, like the one obtained here for zero lean. Incidentally, the reason the other curves are not symmetric about  $\alpha = 0$  is simply due to the fact that with a constant positive lean  $\theta$  the steering leads either on the correct side ( $\alpha > 0$ ) or on the wrong side ( $\alpha < 0$ ) of the lean.

The observed minimums can be seen experimentally. At rest, when the frame is tilted, the front-fork assembly rotates into the lean to the corresponding minimum of the bike's gravitational potential energy. But, as we shall see later, these minimums represent highly unstable riding conditions.

The conclusion is obvious: geometry alone does not provide the right potential curves. But can we ignore the main dynamical contribution?

### Dynamical Equilibrium

The gyroscopic forces on the wheels - on the order of a few newtons for modern wheels - were studied by Klein and Sommerfeld, who found them negligible and unable to account for the equilibrium. However, by inducing the correct centrifugal force, these forces do contribute to the stability of the riderless bike and enable a rider to ride "hands off" - when the rider's weight lies mostly on the back wheel and the reduced ground friction of the front wheel allows it to swivel freely.

However, the centrifugal force itself can be taken into account by computing the height of the fork point subject to condition (1). The results of the calculations are shown on Figure 4 for different values of the speed  $v$  (with the same ordinates as above) versus the turn angle  $\alpha$ . As expected, the curves about  $\alpha = 0$  are (i) symmetric and (ii) not too peaked; i.e., the instability is not too dramatic, and fall can easily be checked by calling on the centrifugal force through proper steering. Conversely, even though constant attention is required by the rider to maintain the center of gravity close to  $\alpha = 0$ , at 9 and 18 km/h (2.5 and 5 m/s) the centrifugal force in a curve with

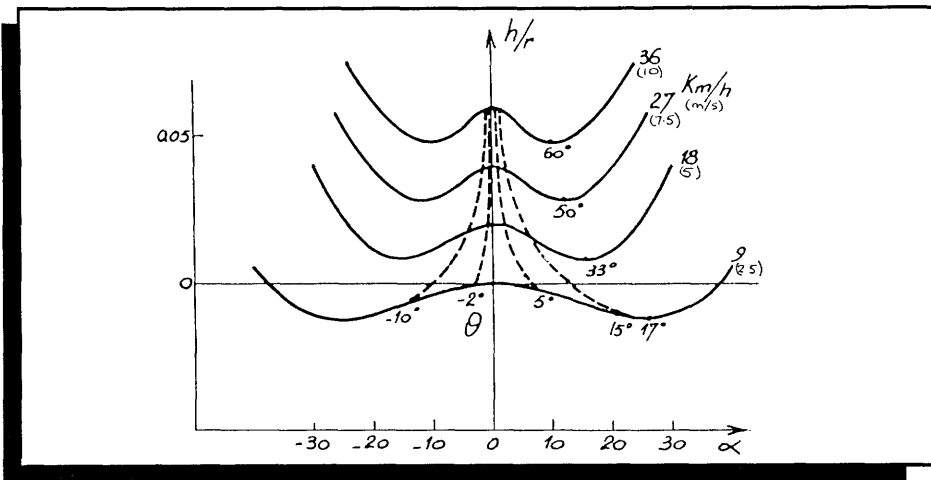


FIG. 4: Dynamical-stability curves for the bicycle of Figure 1 are shown at different speeds, given in km/h and m/s. The same ratio  $h/r$  is plotted versus the turn angle  $\alpha$  in degrees. Again, the curves have been shifted vertically for clarity. Constant lean angles  $\theta$  are shown in dashed lines, as well as the lean in the minimums; these are of course symmetric about  $\alpha = 0$ .

a  $\alpha = 5^\circ$  can be offset easily by a lean of  $3^\circ$  and  $12^\circ$  respectively. This time, of course, the lean angle increases either with the speed or the turn angle, as it should.

The stability curves become more peaked as the speed increases but, due to the  $v^2$  dependence of the centrifugal force, a given lean angle can be offset by a smaller steering angle, as shown by the dotted curve in Figure 4. This gives the feeling, which Jones sought to explain, of greater stability at high speed. Other stabilizing effects, such as gyroscopic forces, trail friction and the corresponding dampening of lateral oscillations do become significant [6, 7].

The trail  $T \equiv TO$ , as shown on Figure 1, is:

$T = (r \cos \chi + 1 \cos \psi) / \sin \chi$ ; it decreases on either side of  $\alpha = 0$  and goes through zero at the minimums.

The derivative,

$$dh/d\alpha = T(\cos \psi \sin \alpha + \sin \theta \sin \psi \cos \alpha) / \sin^2 \chi;$$

cancels either for  $T = 0$  or for  $\alpha = 0$ . This explains the stability around  $\alpha = 0$ . However, the trail  $T$  changes sign at either minimum where the front wheel may then switch spontaneously backwards to the negative trail or "unridable" bike of Jones.

Figure 5 shows how the stability curves are modified around the equilibrium  $\alpha = 0$  by the trail length  $T$ : the longer the trail, the harder the rider will have to hold the handlebars against

further turning, as shown by the (negative) increase of the second derivative.

The consequences for steering-fork design are obvious. With a small trail ( $T = 20$  to  $30$  mm), the bicycle will not lose too much of the high responsiveness particular to the zero trail, will still benefit from the stabilizing caster effect, and will have the dangerous minimums distant enough from  $\alpha = 0$  for all practical purposes. Even if empirical efforts have already led to satisfying results, the present theory may help to improve design. As can be seen from Figure 5, when the trail length is kept constant, the fork angle has practically no effect on stability. Consequently, builders may choose the fork angle subject only to mechanical constraints, and then choose the trail length according to the desired steering flexibility.

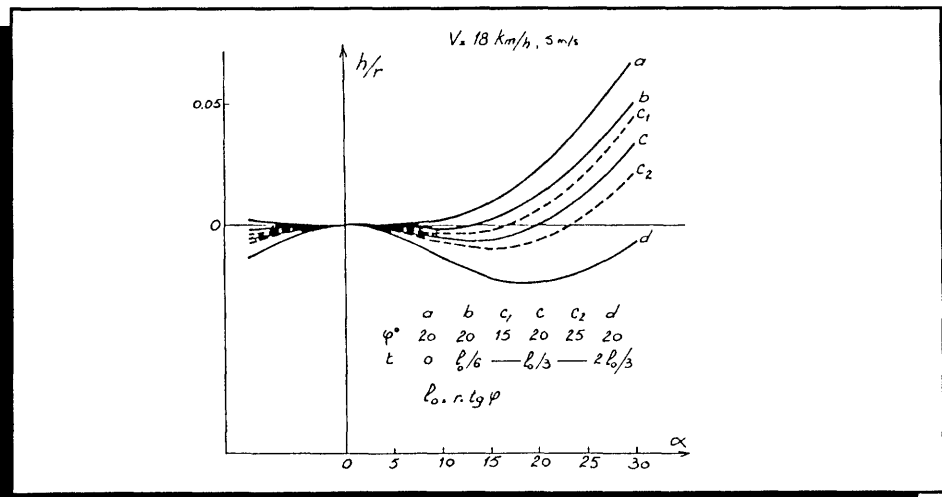


FIG. 5: Variation of stability curves. Stability-curve variation is shown near the equilibrium at  $\alpha = 0$ , as a function of fork angle and/or trail length  $T$ .

### Acknowledgements

The author wishes to acknowledge useful correspondence with Prof. D. Jones and enlightening discussions with Prof. A. Berroir and P. Vernin.

### References

- [1] McGaw, G., *Engineer* (London), vol. 30, December 2, 1898.
- [2] Carvallo, E., Théorie du mouvement du monocycle et de la bicyclette, *Journal de l'Ecole Polytechnique*, 2e Série, Cahiers 5 et 6, 1901.
- [3] Klein, F. and Sommerfeld, A., *Theorie des Kreisels*, Vol. IV, ch. IX-8, Teubner, Leipzig, 1910.
- [4] Douglas Roland, R., *Computer Simulation of Bicycle Dynamics*, Calspan Corp., Buffalo, N.Y.
- [5] Jones, D., The stability of the bicycle, *Physics Today*, p. 34, April 1970.
- [6] Lowell, J. and McKell, H., The stability of bicycles, *Am. J. Phy.* 50, p. 1106, December 1982.
- [7] Rocard, Y., *Théorie générale des vibrations*, 128, Masson, Paris, 1971.

**Y. Le Hénaff**  
**49 rue de Chatenay-G3**  
**Antony 92610-FRANCE**

## Discussion of Le Hénaff's Paper

By Jim Papadopoulos and  
Andy Ruina

Even a bicycle in a steady turn, the subject of Le Hénaff's interesting paper, is difficult to analyze. This is immediately revealed by a glance at the extremely complicated equations in ref. (2). Deep understanding can only come from the use of idealizations like those implied by Le Hénaff: assuming a concentrated mass at the CG point; and neglecting gyroscopic effects, deformation of the bicycle, and dissipative friction. Although Le Hénaff's assumptions cannot be used to predict all bicycle phenomena, they seem appropriate for estimating and understanding the potential energy of handlebar torque in steady turns.

However, such quantities calculated from steady equilibrium motions may have only *subtle* connections to what would be called "stability" – either by a bicycle rider or by a student of the bicycle as a *dynamical system* (where the change of lean and steer-angle with time are governed by differential equations.)

Consider as a special case the dynamical stability of a bicycle with no rider. Call a bicycle "stable" if it recovers to steady straight-ahead motion after any small disturbance from that motion, and "unstable" otherwise.

Surprisingly, for a range of speeds, many bicycles are "stable" in this sense. Mathematical analyses and experiments both indicate, opposing some intuitions, that this "stability" is only possible for a bicycle if its Le Hénaff curves (modified as illustrated) are "peaked" (concave down) in the center. For such a bicycle in a steady turn, the handlebars need to be held against further turning! (However, if there is a rider, this torque is greatly altered when he/she bends sideways.)

The intuitive assumption that stability is synonymous with a potential-energy minimum does not apply to a moving bicycle, which has finite kinetic energy, gyroscopic forces, and non-holonomic constraints [see refs (1), (3)]. One must be wary of stability arguments that do not take into account the appropriate *dynamical* (time varying) equations of unsteady motion.

Incidentally, to calculate handlebar torque during steady turns, probably slightly different quantities should be plotted in Le Hénaff's figures 4 and 5. The vertical axis should plot (*the CG's distance from the line between the front and rear-wheel contact points*)/ (*the cosine of the angle of lean of the plane containing the CG and the two contact points*). The horizontal axis should plot the steer angle  $S$ . The handlebar torque for a given steer angle  $S$  will be proportional to the slope of this curve at

$S$ , plus gyroscopic terms. (Such modified curves will be generally similar to those in figure 4. But in contrast to figure 4, the "peakedness" of the curves – the 2nd derivative evaluated at  $S=0$  – should probably not depend on rider speed  $v$ .) Plotted in this fashion, for example, a bicycle with vertical head angle and non-zero trail would always make a "valley".

We appreciate Le Hénaff's work on bicycle equilibrium and stability, and hope he continues his investigations.

### References

1. Gray, Andrew (1918) *A Treatise on Gyrostatics and Rotational Motion*; republished by Dover in 1959. (See pp. 19-20 and 29-33.)
2. Man, G.K. and Kane, T.R., *Steady Turning of Two-Wheeled Vehicles*; in **Dynamics of Wheeled Recreational Vehicles**, SP-443, Proceedings of 1979 SAE Congress in Detroit, pp. 55-75.
3. Neimark, J.I. and Fufaev, N.A. (1967) *Dynamics of Non-holonomic Systems*; translated from Russian and published in 1972 by the American Mathematical Society, Providence R.I., (See pp. 330-374.)

**Cornell Bicycle Research Project  
Theoretical & Applied Mechanics  
Thurston Hall  
Cornell University  
Ithaca, NY 14853  
(607) 255-5035**

## The Author Responds...

- Whipple is certainly a good reference if I judge by hearsay. Unfortunately, I could not get a copy of Whipple's old paper. Can you send me a copy? Same with Neimark & Fufaev's relevant pages. Now, as for why my analysis, I thought it was plain from the subtitle of D. Jones' paper. Besides, Jim provided some of the answers between the brackets.

- Front-wheel/fork vibrations have nothing to do with equilibrium; they are related to what engineers call shimmy or wobble of wheels. These vibrations obey two coupled differential equations (see my ref. 7) in which the trail has a dampening effect only. I ex-

perienced them once, going down a slope with a loaded front fork; they are very impressive.

- I agree, I mean equilibrium. And, according to Lagrange's theorem (in *The Stability of Motion* by N. Chetayev, Pergamon, 1961, p. 32), "if, in the equilibrium position the potential function has an isolated maximum, then this equilibrium position is stable." So, of course, are the two minimums. However, as I show later, the trail (of a non-zero-trail bike) will not change sign at the maximum, contrarily to what happens to the minimums with, eventually, dramatic consequences on 'stability.'

- The reason I worked again the height of the fork point is two-fold, besides the fact that it is a good way to get at the c. of g. First, because Jones himself was not sure of his calculations (cf. his subtitle!), inasmuch as it gave him 'absurd' and 'unphysical' results – his own words. His doubts stemmed from the fact that he solved the geometry for an infinitely long bike (a fact I found only after my own calculation, confirmed later by him) and got wrong potential curves. Second, I wanted to see whether I could get the correct curves with a normal-length bike. Now, the reason this height has to be computed in the frame plane (in the plane of the bike, said Jones) is for a

POINT/COUNTERPOINT/POINT/COUNTERPOINT/POINT/COUNTERPOINT/POINT/COUNTERPOINT

dynamical reason. When a pendulum is swept around on a circle, the dynamical stable position is when its c. of g. is lowest along the supporting line. i.e. in the moving frame, not in the lab.

- The first reference (Am. J. of Physics) rejected my paper because, wrote the reviewer, "[I] doubt that a bicycle possesses an inherent stability." Now, with Jim, I have come all the way around: he argues the bicycle is intrinsically stable. I doubt anyone can make a [short] article semantically fool-proof and I [plead] for a minimum of fairness from the reader. When Jim argues that an unmoving bicycle 'supported against tilting' is stable, there is no doubt about it. Now, what will happen if it is not supported anymore?

Static or moving, the area of the polygon of support of a bike is zero (line between front and rear-wheel ground contacts). Notwithstanding the gyroscopic forces Jim refers to, equilibrium has to be learned. This is what I mean by intrinsically unstable. I agree that gyroscopic forces play a role (in no-hands riding); so does the shift of the line of support left or right when the front wheel turns (in static, standing equilibrium), but they are minor compared to the centrifugal force. It is difficult to ride hands-off when the front wheel is heavily loaded and inertia and the Coulomb (friction) force between ground the front tire overload the gyroscopic effect. Similarly, the second effect will be absent on a zero-trail bike which is nonetheless perfectly rideable, if not so leisurely, hands off.

But I will not argue with Jim about a point on which we agree: under proper dynamical conditions, a moving bike (faster than, say, about 1 m/sec for a riderless bike) with or without rider is stable according to my potential curves and [the wording of] Lagrange's theorem.

- Should the potential maximum be broad? Neither ... Now tell me, how broad is broad? The zero-trail bike has what I call a broad maximum. Yet, it is not called stable because it is difficult to ride hands-off (any bump on the road

may turn the wheel around). Positive trail acts as a spring to straighten the front wheel of a forward-going bike; no wonder a negative spring will compensate this effect on a negative-trail bike. How broad is also a matter of personal taste. Short-trail bikes are easy to ride but, for straight-line races, people prefer long trails so that they can forget the steering and concentrate on speed.

- To my knowledge, bikes have little frictional torque except for the front-wheel ground contact compounded by side effects of the trail. Were it not for this, on a zero-trail bike, the derivative of my potential curve with respect to  $\alpha$  would indeed give the handlebar torque. But it is not so easy to take this friction into account and, moreover, on a positive-trail bike, one would have to take into account the straightening effect of the trail. This is the reason I cannot simply identify the derivative with the handlebar torque, although it is roughly so.

- I have not read Sharp's calculations but I would appreciate a copy.

In summary, I do not claim the problem is solved in full generality. Remember, the bike is a doubly non-holonomic system with five degrees of freedom (three only in infinitesimal motion, one of them being the rotation of the rear wheel in its instantaneous plane, which is of course not taken into ac-

count here), that is excluding the degrees of freedom of the rider himself, for which classical equilibrium theories from Lagrange's to Liapunov's are of little help.

But I claim to have made substantial progress on the equilibrium theory of the bike, inasmuch as it is the first time we have realistic potential curves showing the equilibrium riding conditions and from which one can infer (my Figure 5) qualitative information concerning the effect of front fork geometry on the handlebar torque.

Jim asks for further calculations. Thanks for his confidence. I may think about it sometime, if, as it stands, this paper is deemed worthy of publication. However, the full theory may not be as clear and accessible [as] Jim would wish it to be, even though it were limited to small angle variations.

You were looking for a common acquaintance. I have found one. Charles Hyde-Wright works with us here on the linac. He read with interest both my article and Jim's criticisms and concluded that we were essentially in agreement except for some minor points of semantics – namely stability/equilibrium. He made several suggestions and, with Jim's criticism, I hope this new version will now be more palatable, if not fool-proof.

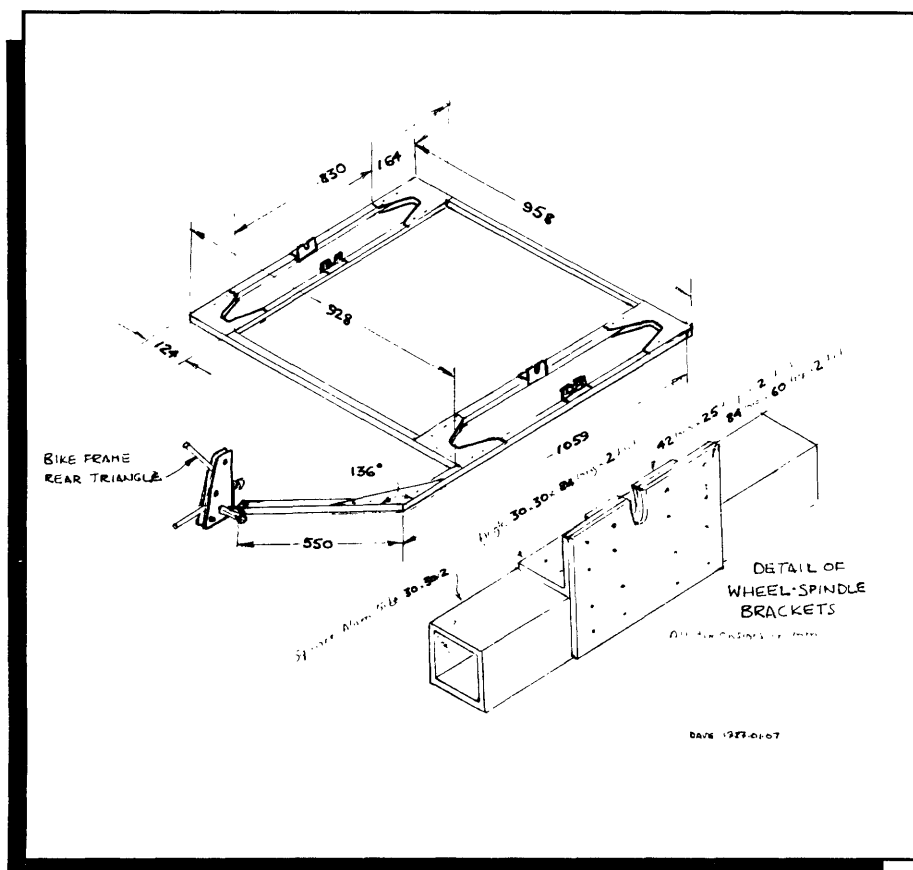
[Editor's note: Charles Hyde-Wright is a former president of the Boston Area Bicycle Coalition and was recently graduated from MIT with a PhD.]

### *Announcing...*

#### The 13th Annual International Human Powered Speed Championships September 23 - 27, 1987 Washington, D.C.

200 Meter Sprints • Practical Vehicle Competition • Watercraft Events • Aircraft Demonstrations • Road Races • All-Terrain Vehicle Display • "Mini" Symposium • Election of Board Members • Annual Membership Meeting  
*for registration packet write:*

IHPVA  
P.O. Box 51255  
Indianapolis, Indiana 46251-0255 USA



Frame of the Flunder Trailer

## Construction of the Flunder Bike Trailer

As mentioned briefly in HP 5/3, Falk Riess and Rainer Pivit of the Bicycle Research Group, University of Oldenburg, West Germany, developed a bicycle trailer that was shown on the North German TV show, "Market of Ideas." There were many requests for their plans, which were distributed at no cost by the TV network. Falk and Rainer gave me a set in Vancouver; we showed an extract in the last HP, requesting help in translation.

Among the several who were kind enough to offer was Otto Brodrick, a recumbent enthusiast working for the government in Ottawa, Canada, and presently spending a year at Harvard. He dictated a translation to a tape recorder. I am giving a highly edited version here, with comments. I am a long-term enthusiast of bicycle trailers for carrying heavy loads for short distances, making my first when I was 13 to supply our WWII victory gardens with water and malodorous varieties of fertilizer. When I returned from two years in Nigeria, I designed a bike trailer for the organization VITA for use in developing countries. It had much in common with Flunder, but

had a regular "push-cart" handle with an attachment behind the saddle, instead of the clever one-sided ball joint near the rear wheel center shown here. Dave Wilson.

### CAUTIONS AND DISCLAIMERS

This design was produced by thorough and conscientious effort by the Bicycle Research Group, but the group cannot be held responsible for any failures in design or performance. It is for individual, not commercial use. Bicycle wheels used in the trailer are not designed to handle side loads so that sharp turns or bumps or riding along a slope should not be attempted with a loaded trailer. I (Dave) will add my own caution that bicycle brakes are often marginal, and to add a heavy, unbraked trailer that can accentuate the tendency to lift the rear wheel off the ground in heavy braking is greatly to reduce one's factor of safety. But used with a great deal of extra care, a trailer can enable one to move loads much greater (e.g. over 50 kg.) than is possible with a regular bicycle alone.

### D.I.Y.

The construction of the frame is illustrated. We leave the design of additions to you. The simplest is a sheet of plywood rivetted to the frame, with loads secured by a web of rubber cords. The frame can be constructed of either aluminum, in which case the trailer will weigh about 8 kg., or steel, weighing about 11 kg. The aluminum construction is shown here.

Materials required include:

- Square aluminum tube, 30x30x2mm - between 1" and 1.25" square, between 1/16 and 3/32" thick - about 6m total length (under 20')
- Aluminum sheet, 250x1000x2mm - say 1' x 3' x 3/32"
- about 350 blind ("Pop") rivets 'type 4x8 with stainless-steel shafts' (e.g. 3/16" x 3/8" long)
- two bicycle wheels of similar diameter to that of the bike
- a small ball-joint coupling, e.g. 20mm (3/4 - 1") diameter;
- a nylon or similar strap (see illustration) to hold the trailer if a fall disengages the ball joint;
- four bolts, nuts and washers, about 6mm (1/4") diameter and 25mm (1") long to bolt the socket part of the coupling to the bike frame;
- glue, e.g. epoxy or acrylic, to use between the joints before rivetting.

[Note: the ball and socket coupling is apparently obtainable in German bike and motor-cycle stores. If you can't get something similar, ingenuity will surely fill the void. I use tennis balls for duties like this. Ed.]

All joints are stiffened by aluminum plate, glued and rivetted as shown on the sketch. The designers set the wheel-spindle dropouts with the openings upwards, partly to lower the center of gravity, and partly to ensure that the users had the wheels on tight. I (Dave) would feel like adding a retainer in case the once-tight spindle became loose.